AN EXPERIMENTAL AND THEORETICAL INQUIRY INTO THE NATURE OF THE STRUCTURES OF HYDROCARBON CATIONS AND THE STRUCTURE AND BARRIER TO ROTATION IN GUANIDINIUM IONS

by

THOMAS D. BERKE

A dissertation submitted to the Graduate Faculty in Chemistry in partial fulfillment of the requirements for the degree of Doctor of Philosophy, The City University of New York.

1974

This manuscript has been read and accepted for the Graduate Faculty in Chemistry in satisfaction of the dissertation requirement for the degree of Doctor of Philosophy.

12/12/74
Date

Chairmen of Examining Committee and

23 Dec 1974
Date

Executive Officer

Supervisory Committee

The City University of New York

CONTENTS

TABLES

FIGURES

FIGURES

ACKNOWLEDGEMENTS

I would like to thank Dr's. A. V. Santoro and J. J. Dannenberg for their guidance and assistance throughout my doctoral career.

I would also like to thank Dr's. D. L. Beveridge and R. Disch for their hours of discussion, and Dr. Beveridge for use of his INDO program.

A very special thanks and deep appreciation is due my wife, Susan, and son, Justin, (to whom this thesis is dedicated) for their patience and tolerance through many husbandless and fatherless weeks during the preparation of this document.

A final note of gratitude is due our friends who assisted in the typing, copying, collating, and innumerable other labors.

PREFACE

My dissertation is divided into two distinct phases. Part one is an INDO level quantum mechanical study of the structure and potential surfaces of the ethyl, 2-butyl and phenylethyl cations.

In the second section the geometry and barrier to rotation of the guanidinium ion were determined by INDO methodology. Nuclear magnetic resonance studies were performed for 2,2-dibenzyl-1-1,3,3,-tetramethyl guanidinium and the 1,1,3,3-tetramethyl guanidinium (TMG) ions.

The dissertation will thus be presented in these two parts.

ABSTRACT

AN EXPERIMENTAL AND THEORETICAL INQUIRY INTO THE NATURE OF THE STRUCTURES OF HYDROCARBON CATIONS AND THE STRUCTURE AND BARRIER TO ROTATION IN GUANIDINIUM IONS

by

THOMAS D. BERKE

ADVISORS: Dr.'s A.V. Santoro and J.J. Dannenberg

The semiempirical INDO method was used to fully optimize the C_2 molecules acetylene, ethylene and ethane. Carbon-carbon bond lengths are found to be shorter than experimental ones.

The potential surfaces of the open and bridged ethyl and 2-butyl cations were studied and plotted by the INDO method. In both cases the results indicate a preference for the "non-classical" (bridged) configuration by 45 Kcal/mole. In neither ion is the open cation a local minimum. The barrier to rotation of a methyl group in the bridged 2-butyl cation was calculated to be 5 Kcal/mole. A comparison of the ethyl and 2-butyl cations offers direct evidence for hyperconjugative stabilization in the latter. A methyl group was found to be a π-donor and σ-acceptor of electron density from its neighboring carbon.

The bridged phenylethyl (phenonium) cation was considered in great detail. Results reveal a great deal of distortion of and charge delocalization into the 6-member ring. The distortion is consistent with a shift in hybridization of the bridging carbon from sp^2 toward sp^3. Charge distribution is consistent with that expected from resonance theory.

The INDO determined barrier to rotation in the guanidinium ion was 24 Kcal/mole. Nmr temperature studies were performed to obtain rotational barrier free energies for 2-benzyl- and 2,2-dibenzyl-1,1,3,3-

tetramethyl guanidinium ions and ortho, meta and para methyl derivatives of the dibenzyl cation. Barriers for dimethylamino and dibenzylamino groups were found to be ca. 15Kcal/mole. Consideration of the Nmr spectra suggests that steric factors cause highly substituted guanidinium ions to be non-planar.

INTRODUCTION

Our intention in undertaking a theoretical study of carbocations was to shed some light on their structures and the nature of their potential surfaces.

Up to the time we began our investigation a great number of experimental studies had been pursued in the area of carbonium chemistry. Their existance was generally accepted in a wide variety of reactions such as Sn1, addition, elimination and rearrangement reactions.[1] Much of the evidence was indirect, i. e. their presence was established based upon kinetic, or other data which did not directly observe these ions. Recent work using proton and ^{13}C NMR, IR, Raman, UV and ESCA spectra have provided direct observations of carbocations and a much better understanding of their structures. Olah has reviewed a great deal of this work.[2]

The first major non-π-electron study of carbonium ions prior to the time we began our work was presented in 1964 by Hoffmann.[3] He used the all-valence electron LCAO MO extended Hückel theory (EHT).[4] The method inadequately treats electron repulsions and yields questionable geometries and charge distributions.[5]

Shortly thereafter, teams working under Pople at Carnegie-Mellon produced three all-valence electron LCAO SCF MO schemes, viz CNDO[6], a reparamaterized CNDO (CNDO/2)[7], INDO[8] and NDDO.[9] These schemes retained important differential overlap terms to varying degrees. The CNDO and closely related INDO methods were extensively tested. Their abilities to predict molecular geometries[9], dipole movements[10], inversion barriers[11], and rotational barriers[12] in good agreement with experiment had been proven. Both produced more reliable restuls than EHT.

On the above basis and on the basis of the economy of operation affording performance of extensive geometric optimizations, we elected to use the INDO method for our carbocation studies. The ability to run extensive geometric searches is important since work done during this period indicated little, if any, geometric optimization had been performed. This was true for Hoffmann's work[3] and other cation studies performed during this period, for example, Sustmann, et.al.[13] and Massa.[14] We wished to know that our optimum structures were produced through an extensive geometry search. We did not want to prejudice our results by determining the best geometry from a choice of several intuitively selected structures.

We have shown that optimization of geometry is critical.[15] Sustmann, et.al.[13] reported a calculation of the ethyl cation in which they assumed the methylene carbon to be sp^2 hybridized, i.e. planar. Our optimization indicates that the methylene hydrogen atoms are actually 3.5° below this plane. We determined the strain energy to be 10 Kcal/mole.[15]

Pople, et.al.[16] further emphasized the importance of an extensive geometric search in a study of the stabilities of $C_3H_7^+$ cations at the ab initio STO-3G[17] and STO4-31G[18] levels. It was discovered that the primary cation, I, was most stable -- a quite unexpected result.

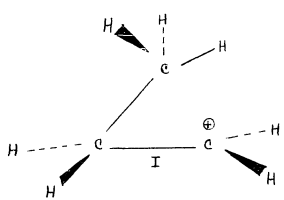

The indicated expected structures were the isopropyl, or protonated cyclopropyl cations. In a later study Pople, et.al. determined the

isopropyl cation to be the lowest energy $C_3H_7^+$ cation.[19]

Another of our goals was to test the ability of the INDO technique to make reasonable predictions for small organic cations. If INDO proves to be a good predictive tool for these simple systems it could then be applied by future researchers with a high degree of confidence to more complex systems.

Dewar, et.al.[20] warn for the extention of molecular orbital techniques into the realm of carbonium ions:

> "All the methods currently available for the study of organic molecules are essentially empirical and can be trusted insofar as they have been tested against experiment. This is just as true for 'ab initio' SCF methods as for semiempirical ones since the errors in the SCF energies are enormous in a chemical sense. If the results of the 'ab initio' calculations are useful this can be so only through a cancellation of errors which cannot be justified on theoretical grounds and can only be established empirically."

Based upon this statement it seems sensible to choose a semi-empirical method which yields good results instead of a higher cost ab initio technique. One of the major difficulties in extending MO methodology to the investigation of carbocations is the paucity of corroborative evidence. Since quantum mechanical results should be expected to correlate with non-solvated, or gas-phase results the rapidly expanding fields of ion cyclotron resonance (icr)[21], such as the recent work by Beauchamp, et.al.[22] on determination of stabilities of carbonium ions, and mass spectroscopy[23] must be looked to to provide such data.

Care must be taken when making correlations with liquid phase data due to the high degree of solvent sensitivity carbonium ions exhibit.[24] A recent article of Schadt and Schleyer[25] indicates an enormous solvent dependence for the ratio of rates of solvolysis of β-phenylethyl tosylate vs. ethyl tosylate. The ratio varied from 0.24 in ethanol to 1770 in the much less nucleophilic trifluoroacetic acid. Such a variation was accoun-

ted for by increased participation of the ß-phenyl group as solvent competition diminishes. Theoretical results will be able to be predictive of condensed phase results if solvation is constant in ions being compared, or along a reaction pathway if a reaction is being considered.

The complete neglect of differential overlap (CNDO)[6], (CNDO/2)[7] and intermediate neglect of differential overlap (INDO)[8] all possess all-valence electron basis sets and are semi-empirical LCAO SCF MO quantum mechanical methods. The approximations applied in the CNDO and INDO methods are essentially identical expect that INDO retains one-center exchange integrals of the form $(\mu\nu|\mu\nu)$, $\phi\mu$ and $\phi\nu$ are on the same atom.[8,26] (This was included to give an adequate account of σ-π interaction so that, for example, ESR hyperfine coupling could be evaluated in terms of spin densities π-density correlation.)[8] For all electron repulsion integrals in CNDO and all except one-center exchange-type integrals in INDO it is assumed $(\mu\nu|\rho\sigma) = \delta_{\mu\nu}(\delta_{\mu\nu}$ is the Kronecker-delta) i.e. zero differential overlap (ZDO)[27] is invoked:

Since the two methods are so similar and since historically CNDO was developed first, CNDO theory will be considered in detail first. INDO theory will then be treated mainly to indicate the ways in which the theories differ.[28]

CNDO[6,7]

The basis set consists explicity of all valence electrons i.e. ls for H, and 2s, $2p_x$, $2p_y$, and $2p_z$ for second period elements. All inner shell electrons and all nuclei are considered as part of a non-polarizable core with which the valence electrons interact.

One-electron molecular orbitals Ψ_i are represented as a linear combination of atomic orbitals (LCAO) ϕ_μ:

$$\Psi_i = \sum_\mu c_{\mu i}\phi_\mu$$

Usage of Slater determinental representation for these Ψ_i produces pro-

perly antisymmetrized wave functions.

Under ZDO[27] and the LCAO approximations the Roothaan equations[29]

$$\sum_{\nu}(F_{\mu\nu} - \varepsilon_i S_{\mu\nu})c_{\nu i} = 0$$

become

$$\sum_{\nu} F_{\mu\nu}c_{\mu i} = \varepsilon_i c_{\mu i}$$

($F_{\mu\nu}$ is the Hartree-Fock, one-electron, Hamiltonian operator, and ε_i is the energy of an electron in Ψ_i).

The Hartree-Fock Hamiltonian operator

$$F_{\mu\nu} = H_{\mu\nu} + \sum_{\rho\sigma} P_{\rho\sigma}\,[(\mu\nu|\rho\sigma) - 1/2\,(\mu\rho|\nu\sigma)]$$

reduces to: Diagonal Terms ($\mu=\nu$):

$$F_{\mu\mu} = H_{\mu\mu} + \sum_{\rho} P_{\rho\rho}\,(\mu\mu|\rho\rho) - 1/2\,P_{\rho\rho}\,(\mu\mu|\mu\mu),$$

or $F_{\mu\mu} = H_{\mu\mu} + \sum_{B} P_{BB}\,(\mu\mu|\rho\rho) - 1/2\,P_{\mu\mu}(\mu\mu|\mu\mu)$ (where P_{BB} is over all atoms B on which ϕ_ρ exist).

Off Diagonal Terms ($\mu\neq\nu$): $F_{\mu\nu} = H_{\mu\nu} - 1/2\,P_{\mu\nu}(\mu\mu|\nu\nu)$ (Where $P_{\mu\nu} = \sum_{i}^{occ} c_{i\mu} \cdot c_{i\nu}$; $P_{\mu\nu}$, $\mu\neq\nu$, is the bond order matrix for ϕ_μ on A and ϕ_ν on B; $P_{\mu\mu}$ is the charge density matrix.)

Thus all three- and four-center electron repulsion integrals of the form $(\mu\nu|\rho\rho)$, $(\mu\mu|\rho\sigma)$ and $(\mu\nu|\rho\sigma)$ are eliminated. Exchange integrals are also neglected.

To assure invariance to linear transformations such as rotation of coordinate axes, hybridization of atomic orbitals, or transformation of the atomic orbital basis set into an equivalent set of symmetry orbitals, the one- and two-center electron repulsion integrals are assigned fixed values which are determined only by the specific atom on which the atomic

orbital resides. The constant is independent of orbital types.

Thus the one-centered coulomb integral, $(\mu\mu|\mu\mu)$, is set equal to γ_{AA} (ϕ_μ on atom A). The two-centered coulomb integral $(\mu\mu|\rho\rho)$ is set equal to γ_{AB} (where ϕ_μ is on A and ϕ_ρ is on B). The Hartree-Fock Hamiltonian simplifies to:

Diagonal terms: $F_{\mu\mu} = H_{\mu\mu} + \sum_B P_{BB}\gamma_{AB} - 1/2\ P_{\mu\mu}\gamma_{AA}$ (ϕ_μ on A)

(where $P_{BB} = \sum_\rho^B P_{\rho\rho}$) i.e. P_{BB} is the total charge density on each atom B).

Off Diagonal Terms: $F_{\mu\nu} = H_{\mu\nu} - 1/2\ P_{\mu\nu}\gamma_{AB}$ (ϕ_μ on A, ϕ_ρ on B.)

Calculation of γ's will be discussed below.

The core Hamiltonian, $H_{\mu\nu}$, treats, among other things, interactions between the valence electrons and their own as well as all other cores. $H_{\mu\mu}$ can be broken down into one- and two-center terms: viz

$H_{\mu\mu} = U_{\mu\mu} - \sum_{B(\neq A)} (\mu|V_B|\mu)$ (ϕ_μ on A).

The two-center term $\sum_{B(\neq A)} (\mu|V_B|\mu)$ describes the attractive force between an electron in ϕ_μ on A with the core of all other atoms B. Again, to retain rotational invariance this is assigned a fixed value, V_{AB}, which is independent of atomic orbital type, and depends only upon the nature of atoms A and B.

$U_{\mu\mu}$ is a one-center term, $U_{\mu\mu} = (\mu|-1/2\nabla^2-V_A|\mu)$. It represents the energy of an electron in ϕ_μ moving in the field of its core. $U_{\mu\mu}$ is evaluated empirically from atomic spectral data (vide infra).

The off-diagonal core Hamiltonian, $H_{\mu\nu}$, equals $U_{\mu\nu} \sum_{B(\neq A)} (\mu|V_B|\nu)$. The two center integral $(\mu|V_B|\nu) = \int\phi_\mu(1)\ r_{AB}^{-1}\ \phi_\nu(1)d\tau$, is similar in form to the overlap integral $S_{\mu\nu} = \int\phi_\mu(1)\phi_\nu(1)d\tau = \delta_{\mu\nu}$ Since in CNDO $S_{\mu\nu} = 0$ if $\mu \neq \nu$ to be consistent $(\mu|V_B|\nu)$ will be set equal to zero. $U_{\mu\nu}$ is zero unless ϕ_μ is on atom A and ϕ_ν is on Atom B. If this is the case $U_{\mu\nu}$ is related to bonding and is retained.

For $H_{\mu\nu}$ in which ϕ_μ is on A and ϕ_ν on B:

$$H_{\mu\nu} = U_{\mu\nu} - \sum_{C(\neq A,B)} (\mu|V_C|\nu) = (\mu|-1/2\nabla^2 - V_A - V_B|\nu) - \sum_{C\ (\neq A,B)} (\mu|V_C|\nu).$$

The last term is set equal to zero for the same reason $(\mu|V_B|\nu)$ above was neglected. The first term $(U_{\mu\nu})$ is not neglected since it allows for energy lowering due to the electron being in the field of atoms A and B. Thus $H_{\mu\nu}$ becomes equal to $U_{\mu\nu}$. $H_{\mu\nu}$ $(=U_{\mu\nu})$ is set equal to $\beta_{\mu\nu}$, the resonance integral, and $\beta_{\mu\nu}$ is then set equal to $\beta^\circ_{AB}\ S_{\mu\nu}$. To allow for invariance to linear transformation β°_{AB} is a constant defined to be dependent only upon atoms A and B and independent of specific orbital type. β°_{AB} is determined empirically (vide infra).

Under these further simplifications the Hartree-Fock matrix reduces to:

Diagonal Terms:

$$F_{\mu\mu} = U_{\mu\mu} + (P_{AA} - 1/2\ P_{\mu\mu})\ \gamma_{AA} + \sum_{B\ (\neq A)} (P_{BB}\ \gamma_{AB} - V_{AB}).$$ (If Q_B is defined as the net charge on atom B, and Z_B the charge of the core of B, then $Q_B = Z_B - P_{BB}$. The diagonal terms can be written:

$$F_{\mu\mu} = U_{\mu\mu} + (P_{AA} - 1/2\ P_{\mu\mu})\gamma_{AA} + \sum_{B(\neq A)} (-Q_B\ \gamma_{AB} + Z_B\ \gamma_{AB} - V_{AB}).$$

The expression $Z_B\ \gamma_{AB} - V_{AB}$ is the penetration integral.[30])

Off-Diagonal Terms: $F_{\mu\nu} = \beta^\circ_{AB}\ S_{\mu\nu} - 1/2\ P_{\mu\nu}\ \gamma_{AB}$ $\mu \neq \nu$

The total energy of a system in CNDO theory can be expressed as a sum of one- and two-center contributions $E_{total} = \sum_A E_A + \sum_{A<B} E_{AB}$ where $E_A = \sum_\mu^A P_{\mu\nu} U_{\mu\nu} + 1/2 \sum_{\mu\nu}^A (P_{\mu\nu}P_{\mu\nu} - 1/2\ P^2_{\mu\nu})$ and, $E_{AB} = \sum_\mu^A \sum_\nu^B (2P_{\mu\nu}P_{\mu\nu} - 1/2\ P_{\mu\nu}{}^2\gamma_{AB}) + Z_A Z_B R^{-1}_{AB} - P_{AA} V_{AB} - P_{BB} V_{BA} + P_{AA} P_{BB} \gamma_{AB}$.

CNDO PARAMETER EVALUATION

CNDO[6] differs from CNDO/2[7] only in the way the core terms V_{AB} and $U_{\mu\nu}$ are evaluated. For this reason description of parametric evaluation for both will be treated simultaneously and when differences arise they will be treated separately.

Using the ZDO[27] condition, $S_{\mu\nu} = \delta_{\mu\nu}$ ($\delta_{\mu\nu}$ is the Kronecker delta) the electron repulsion integrals reduced to γ_{AA} $\{(\mu\nu|\mu\nu)\}$ for 1-center terms and γ_{AB} $\{=(\mu\mu|PP)\}$ for 2-center terms. These constants are evaluated by assuming ϕ_μ and ϕ_p are valence shell s orbitals on atom A (s_A) and B (s_B) respectively. The integrals $(s_A s_A|s_A s_A) = \gamma_{AA}$ and $(s_A s_A|s_B s_B) = \gamma_{AB}$ are integrated using appropriate, i.e. 1s or 2s, Slater-type s atomic orbtial functions.

In both versions of CNDO the one-center portion of the core Hamiltonian is evaluated from spectroscopic ionization data. Since $S_{\mu\nu} = \delta_{\mu\nu}$ and since all one-center repulsion integrals are set equal to γ_{AA} dependent only upon the nature of A, all electron states arising from a particular electron configuration will be degenerate e.g. the ^3P, ^1D, ^1S states from the carbon $1s^2 2s^2 2p^2$ configuration. In the original CNDO version[6] the energy corresponding to a particular state is taken as a multiplicity weighted average of all electron spin states. For an element X (Li to F) the energy is expressed as: $E(X, 2s^m, 2p^n) = mU_{2s2s} + nU_{2p2p} + (m + n)(m + n - 1)\ \gamma_{AA}$. Ionization from this $2s^m\ 2p^n$ configuration can result

from a loss of either 2s or 2p electron. The corresponding energy for each of these states is represented:

$$E_s\ (X^+,\ 2s^{m-1},\ 2p^n) = (m-1)\ U_{2s2s} + mU_{2p2p} + (m+n-1)\ (m+n-2)\ \gamma_{AA}$$

$$E_p\ (X^+,\ 2s^m,\ 2p^{n-1}) = mU_{2s2s} + (n-1)\ U_{2p2p} + (m+n-1)\ (m+n-2)\ \gamma_{AA}$$

The ionization potentials for the above atoms are the differences in energy between the atoms and their appropriate ionization state, viz:

$$I_s = E(X,\ 2s^m,\ 2p^n) - E_s\ (X^+,\ 2s^{n-1},\ 2p^n)$$

$$= U_{2s2s} - (m + n - 1)\ \gamma_{AA}$$

$$I_p = E(X,\ 2s^m,\ 2p^n) - E_p\ (X^+,\ 2s^m,\ 2p^{n-1})$$

$$= -U_{2p2p} - (m + n - 1)\ \gamma_{AA}$$

The one-center core Hamiltonian terms, $U_{\mu\mu}$, thus becomes $U_{2s2s} = -I_s - (m + n - 1)\ \gamma_{AA}$ and $U_{2p2p} = -I_p - (m + n - 1)\ \gamma_{AA}$. For hydrogen ϕ_μ is the 1s orbital, $U_{\mu\mu} = U_{1s1s}$ is taken to be -13.06eV, the value corresponding to the STO with $\zeta = 1.2$, rather than being evaluated empirically.

In CNDO/2[7] the procedure for evaluating $U_{\mu\nu}$ was modified to take into account electron affinity, A_μ, as well as ionization potential, I_μ.

$$-I_\mu = U_{\mu\mu} + (Z_A - 1)\ \gamma_{AA}$$

$$-A_\mu = U_{\mu\mu} + Z_A\ \gamma_{AA}$$

The average of these two expressions yields:

$$-1/2\ (I_\mu + A_\mu) = U_{\mu\mu} + (Z_A - 1/2)\ \gamma_{AA}$$

The core values are then evaluated from:

$$U_{\mu\mu} = -1/2\ (I_\mu + A_\mu) - (Z_A - 1/2)\ \gamma_{AA}$$

The off-diagonal, 2-center elements of the core Hamiltonian, $H_{\mu\nu}$, the resonance integrals are of the form $H_{\mu\nu} = \beta^\circ_{AB} S_{\mu\nu}$. β°_{AB} is expressed as the average of two terms each of which depends solely on the nature of the elements A and B, viz:

$\beta^\circ_{AB} = 1/2 (\beta^\circ_A + \beta^\circ_B)$, and $H_{\mu\nu} = 1/2 (\beta^\circ_A + \beta^\circ_B)$.

The β°_M are adjusted to attain best agreement between CNDO and minimal basis set ab initio LCAO SCF calculations.

The core-attraction integral parameter, V_{AB}, represents the attractive potential between an electron in atomic orbital ϕ_μ on atom A with the core of atom B. The atomic orbital ϕ_μ is assumed to be a valence s Slater-type orbital, and Z_B, the charge of the core of B, is assumed to be a point charge at the center of atom B. Thus V_{AB} can be evaluated from:

$$V_{AB} = \sum_{B(\neq A)} (\mu|V_B|\mu) = \int \phi_\mu(1) Z_B r_{1B}^{-1} \phi_\mu(1) d\tau_1 = Z_B \int s_A^2(1) r_{1B}^{-1} d_\tau.$$

In CNDO/2 V_{AB} is set equal to $Z_B \gamma_{AB}$; no theoretical justification was offered.[7] This approximation was invoked to eliminate a "penetration effect" which led to bond lengths which are too short and binding energies which are too high for diatomics. It also led to predictions of binding energies even when the bond order between the atoms was zero. This means that for the diagonal terms in the Fock-matrix

$$F_{\mu\mu} = U_{\mu\mu} + (P_{AA} - 1/2 P_{\mu\mu}) \gamma_{AA} + \sum_{B(\neq A)} (P_{BB} - Z_B) \gamma_{AB} + \sum_{B(\neq A)} (Z_B \gamma_{AB} - V_{AB})$$

the last term $Z_B \gamma_{AB} - V_{AB}$ is then equal to zero, i.e. the penetration integral is neglected.

The Hartree-Fock Hamiltonian for the more widely used CNDO/2 is:

Diagonal Terms:

$$F_{\mu\mu} = -1/2 (I_\mu + A_\mu) + [(P_{AA} - Z_A) - 1/2 (P_{\mu\mu} - 1)] \gamma_{AA} + \sum_{B(\neq A)} (P_{BB} - Z_B) \gamma_{AB}.$$

Off-Diagonal Terms: $1/2 (\beta^\circ_A + \beta^\circ_B) S_{\mu\nu} - 1/2 P_{\mu\nu} \gamma_{AB}$

An interative process must be used to solve the Roothaan equations[29] $\sum_{\nu}(F_{\mu\nu} - \varepsilon_i) C_{i\mu} = 0$ since $F_{\mu\nu} = F(P_{\rho\sigma})$ and since the bond order matrix can only be specified once $C_{i\mu}$'s are known i.e. the Roothaan equations have been solved. The process works as follows:

a. A Huckel-type estimate of the Fock matrix is used to solve

$F_{\mu\mu}^{(0)} = -1/2\ (I_\mu + A_\mu)$

$F_{\mu\nu}^{(0)} = \beta^\circ_{AB}\ S_{\mu\nu}$

for an initial set of coefficients $(c_{i\mu})$.

b. The coefficients are used to calculate the bond order matrix which is used to calculate a new $F_{\mu\nu}$.

c. The new $F_{\mu\nu}$ is used to calculate another set of coefficients.

Steps b and c are repeated until, in the version we used, the electronic energy agrees in two successive iterations to within 10^{-7} a.u.

THE INDO FORMALISM

The INDO method[8] differs from CNDO is that one-center exchange integrals of the type $(\mu\nu|\mu\nu)$, where ϕ_μ and ϕ_ν are on the same atom, are retained. This allows for better calculated spin densities and thus ESR hyperfine coupling constants.[8,26]

Under the INDO formalism the closed-shell Fock Hamiltonian becomes

Diagonal terms:

$F_{\mu\mu} = U_{\mu\mu} + \sum_{\rho} [P_{\rho\rho}(\mu\mu|\rho\rho) - 1/2\ P_{\rho\rho}(\mu\rho|\mu\rho)] + \sum_{B(\neq A)} (P_{BB} - Z_B)\gamma_{AB}$

(ϕ_μ on atom A)

Off-Diagonal Terms:

$F_{\mu\nu} = 1/2\ P_{\mu\nu}\ [3(\mu\nu|\mu\nu) - (\mu\nu|\nu\nu)]$. ($\phi_\mu$ and ϕ_ν both on A)

$F\mu\nu = 1/2\ (\beta^\circ_A + \beta^\circ_B)\ S_{\mu\nu}$ $1/2\ P_{\mu\nu}\gamma_{AB}$ {ϕ_μ on A, ϕ_ν on B}.

The one-center repulsion integrals are expressed using Slater-Condon parameters:[31]

$(ss|ss) = (ss|xx) = F^\circ = \gamma_{AA}$ where s=2s, x=2p_x, y=2p_y, z=2p_z

$(sx|sx) = 1/2\ G^1$

$(xy|xy) = 3/25\ F^2$

$(xx|xx) = F^\circ + 4/5\ F^2$

$(xx|xx) = F^\circ + 4/5\ F^2$

$(xx|yy) + F^\circ - 2/25\ F^2$

plus similar expressions for $(ss|zz)$, etc., F°, γ_{AA} is evaluated as in CNDO theory using a valence shell Slater-type s orbital. G^1 and F^2 correspond to the values determined empirically by Slater[31] to best fit atomic spectral data.

The evaluation of the one-center interaction terms $U_{\mu\mu}$ is similar to the original CNDO[6] method with inclusion of G^1 and F^2 terms:

$E(X, 2s^m, 2p^n) = mU_{2s2s} + nU_{2p2p} + 1/2\ (m + n)\ (m + n - 1)\ F^\circ - 1/6\ mnG^1 - 1/2s\ n(n - 1)\ F$. As in CNDO I_μ, ionization potential, and A_μ, electron affinity, values are determined from appropriate energy differences. The following relationships between $1/2\ (I_\mu + A_\mu)$ and $U_{\mu\mu}$ are determined:

Hydrogen: $-1/2\ (I_s + A_s) = U_{1s1s} + 1/2\ F^\circ$

Lithium: $-1/2\ (I_s + A_s) = U_{2s2s} + 1/2\ F^\circ$

$-1/2\ (I_p + A_p) = U_{2p2p} + 1/2\ F^\circ - 1/12\ G^1$

Beryllium: $-1/2\ (I_s + A_s) = U_{2s2s} + 3/2\ F^\circ - 1/2\ G^1$

$-1/2\ (I_p + A_p) = U_{2p2p} + 3/2\ F^\circ - 1/4\ G^1$

Boron to Fluorine:

$$-1/2\ (I_s + A_s) = U_{2s2s} + (Z_A - 1/2)\ F^0 - 1/6\ (Z_A - 3/2)\ G^1$$

$$-1/2\ (I_p + A_p) = U_{2p2p} + (Z_A - 1/2)\ F^0 - 1/3\ G^1 - 2/25\ (z_A - 5/2)F^2$$

All other details are the same as for CNDO/2.[8]

DISCUSSION

CNDO and INDO theories have been extensively tested. (For an annotated survey of a great deal of this literature see the book by Pople and Beveridge.[28a]) These techniques have found success in predicting molecular geometries[9], dipole movements[10], inversion barriers[11], and rotational barriers[12] for hydrocarbon as well as for heteroatom species. They have been successfully applied to calculations of NMR phenomena.[32] INDO has been shown to reproduce ESR data better than CNDO.[28a] CNDO does not adequately account for σ-π interactions thus yields poor descriptions of spin densities in σ orbitals.[8] INDO has also been able to account for differences in energy in various spin states arising from the same ground state electron configuration.[6]

Snyder in a study of the 2-phenylethyl to phenomium cation coversion[33] showed that CNDO/2, and presumably INDO, favors three-membered ring structures over their straight chain isomers (see table 1). CNDO is seen to favor the thermodynamically less stable 3-member cyclic compounds. Small basis set ab initio calculations show a similar bias.[35] A larger basis set ST06-31G ab initio calcuation by Hariharan and Pople[36] shows a bias against 3-member rings predicting them to be relatively less stable than they are. Table 1 indicates that inclusion of polarization (d-orbital type) functions stabilizes ring structure more than their straight chain isomers.[36, 38, 39]

In a study of the relative stabilities of the open vs. bridged ethyl cation, $C_2H_5^+$, (see table 2) Pople, et. al.[38] again indicate that the addition of polarization functions stablizes the bridged structure more than the open isomer. In this case the bridged cation becomes more stable than the open. They state that the bridged cation may well be the favored

COMPOUND	CNDO[a]	STO-3G[b]	ST06-31G[c]	ST06-31G[d]
Propene[e]	-24.7513	-115.66030	-117.02768	-117.07111
Cyclopropane[e]	-24.8995	-115.66616	-117.00777	-117.05872
Allyl Cation[f]	-23.4513	-----	-----	-----
Cyclopropylcation[g]	-23.5809	-----	-----	-----

a.) Using Wiberg's parameters, ref. 34

b.) See ref. 35

c.) See ref. 36

d.) As (c) except d-functions were added

e.) Parameters from ref. 37

f.) Assumed planar, r(CC) = 1.408 Å, r(CH) = 1.08, all angles 120°

g.) The same structural parameters as cyclopropane except the cations center is assumed planar.

Table 1. Total energies (hartrees) for C_3 hydrocarbons and cations.

METHOD	INDO[a]	STO6-31G[b]	STO6-31G[c]	IEPA[d]
ΔE^{e}	+0.0734	-0.01026	+0.00011	+0.0140

a.) This work

b.) See ref. 36

c.) Same as b with d-type polarization functions included

d.) Correlation energy study. Independent-electron pair PNO See ref. 40

e.) $\Delta E = E$ (bridged) - E (open)

Table 2. Relative energy (hartrees) of bridged vs. open ethyl cations.

structure in the Hartree-Fock limit.[38] They also mention that relative correlation energies for bridged vs. open isomers may have a marked effect on their relative stabilities.

Zurawski, et. al.[40] studied the effects of correlation on three-member ring structures. For the ethyl cation they discovered that correlation errors were greater in the bridged structure than in the open structure.

Correlation corrections further stabilizes the bridged structure in ab initio calculations (see table 2). Thus as corrections are added to compensate for basis set limitations and for neglect of correlation in ab initio methods the three-member ring species gain greater stability than their open isomers.

OPTIMIZATION TECHNIQUE

The method used to obtain the optimum energy structure for each of the cations studies will be described in this section in detail so that it need not be reiterated for each optimization. Specific geometric constraints for each ion will be dealt with in the appropriate section.

The description below retraces the path from the initial geometry to the optimum configuration.

The first of the two portions of the process involves variations of each parameter "crudely" i.e. bond lengths were varied by large increments usually 0.05Å for CC bonds, 0.005Å for CH, and angles were also varied using fairly large intervals from small up to large values.

Bonds with little angular dependence e.g. C=C in ethylene or C_2 - C_3 bond in the 2-butyl cation were varied independently. Bonds with included angles, such as CH bonds in ethylene or ethane, were varied crudely in "Do-Loop" fashion, i.e. a range of bond lengths were tested at various angles to find the best combination.

After approximate best angles and bond lengths are determined from the above procedure the final phase of optimization is undertaken. All parameters are varied dependently in a "Do-Loop" around the determined "best" values over smaller increments and much smaller ranges than the first variation. The final optimization is run after this procedure converges on an overall optimum structure. The purpose of the final optimization is to define all parameters to the desired precision. For bonds to carbon this was 0.01A°, bonds to hydrogen - 0.001A°. Bond angles are accurate to 0.1°.

The first carbocation we studied was the ethyl cation since it is the simplest one which can exist in an open ("classical"), II, or bridged ("non-classical"[41]), III, configuration. The relatively low cost per calculation afforded by the INDO technique and the simplicity of the ion makes it feasible to do a total optimization of all the parameters in the system as well as a full study of the potential surface for ethyl cation. This is important for two reasons: (1) both the pathway for protonation and the barrier to hydride shift can be determined, and (2) full geometric optimization can be critical as pointed out in the introduction.

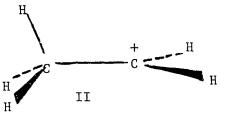

II

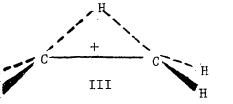

III

The ethyl cation has been the subject of a large number of studies. Roberts and Yancey[43] generated the C^{14}-labeled carbonium ion by deamination of ethylamine-1-C^{14} in aqueous medium with perchloric acid and sodium nitrite.

In the product only 1.5% of the rearranged alcohol (ethanol-2-C^{14}) was formed indicating that the open cation, II, reacts with water more rapidly than it can be converted to the bridged cation, III, and more rapidly than an equilibrium of the two degenerate ions, II (C^{14}) and

$$\underset{\text{II}(C^{14})}{CH_3C^{14}H_2^+} \rightleftharpoons + \underset{\text{IV}}{CH_2C^{14}H_3}$$

IV can occur.

Myhre and Evans[44] indicate that under appropriate choice of solvent the anchimerically assisted pathway becomes favored over the solvent assisted pathway. They generated the 1,1-dideuteroethyl cation by action of fluorosulfonic acid on ethyl tosylate and observed 42% rearrangement.

Differences in these results may well be attributable to a difference in solvent systems. Carbonium ion reactions are known to exhibit a high degree of solvent sensitivity.[24] Schadt and Schleyer[25] performed a quantitative study of the solvent dependence of the relative rates of solvolysis of β-phenylethyl tosylate and ethyl tosylate. The ratio varied from 0.24 in ethanol to 1770 in the much less nucleophilic more strongly ionizing trifluoroacetic acid. The study indicated that the anchimerically formed phenonium ion becomes favored as competition from the solvent decreases.

Shiner[45] noted a non-cumulative β-deuterium isotope effect in the solvolysis of deuterated 2,4-dimethyl-3-pentyl brosylates suggesting neighboring group participation in the transition state. Shriner's rate data on the solvolysis of β-deuterated 4-t-butylcyclohexyl brosylates also suggested neighboring group assistance.[46]

Evidence for the existance of the bridged 2-butyl cation, V, as an intermediate in the trifluoroacetolysis of 2-butyl tosylate was reported from this lab.[47]

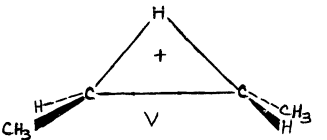

V

Trifluoroacetolysis of 1,1,1,2-tetradeutero, VI, and 3,3,4,4,4-pentadeutero-2-butyl tosylates, yielded equal amounts of their major products VIII and IX, and XII and XIII respectively. Compound VI reacts

more rapidly than X as would be expected based upon a β-deuterium isotope effect if neighbor participation were important in the reaction mechanism. The participation of a bridged intermediate is also evidenced by the approximately equal amounts of VIII and IX produced from VI and predominance of products XII and XIII from X. If the pathway involved rapidly equilibrating ions XIV a-d then products VIII and IX, and XII and XIII would be present to a much lesser extent than they were, viz. 94% and 73% respectively.

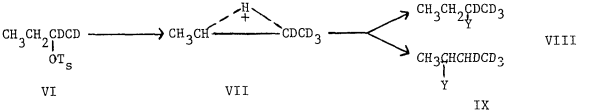

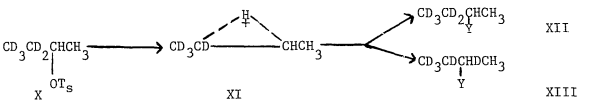

Y=Trifluoroacetate

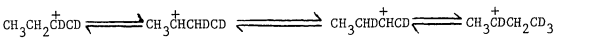

XIVa XIVb XIVc XIVd

Gas phase studies eliminate solvent effects and hence should be expected to be more consistent with theoretical results. A recent ion cyclotron resonance study of the decomposition of diethyl-n-nitrosoamine by Jaffe and Billets[21c,d] indicates that only D^+ was lost from $CD_3CH_2^+$ to form $CD_2=CH_2$ upon attack by a base. This seems to indicate a deuterium

bridged structure, or an open cation which loses D^+ more rapidly than equilibration between $CD_3CH_2^+ \rightleftharpoons CD_2CH_2D^+$ can occur.

Ausloos, et.al[23c] indicate that the barrier for the hydride shift must be less than 5 Kcal/mole. In this mass spectral study of the decompositions of $CD_3CH_2I^+$, $CH_3CD_2I^+$ and $CD_3CH_2Br^+$, it was determined that they all produced about 90% of the scrambled product CD_2HCDH_2. This could be explained by rapidly equilibrating cations or by a bridged pathway. The discrepancy between these studies suggests further experimentation is necessary to determine conclusively the relative stability of the ethyl cation in the gas phase.

Differences between Jaffe's and Ausloos' results may be due to the fact that vibrationally excited molecules possess sufficient interval energy to overcome barriers to hydride migration.

Due to the size of the ethyl cation many theoretical studies have been carried out on the system.[3,13-16,20,38,40,48,49] Semiempirical results usually favor the bridged structure, III. Ab initio methods generally favor the open isomer, II. As mentioned in the theoretical section (q.v.) inclusion of polarization functions[38] as well as corrections for correlation effects[40] stabilizes the bridged cation more than the open. For the ethyl cation this leads to a more stable "non-classical"[41] structure. (These results will be considered in more detail in the results and discussion section for the ethyl cation, vide infra).

REFERENCE SYSTEMS

Before undertaking an in depth study of the ethyl cation, II and III, we desired to provide reference systems against which we could compare our cation results. Since no experimental geometric data is available on these ions such a study is mandated. We chose a system containing only sp^2 hybridized carbons in a double bonded system, ethylene, and

one containing only sp^3 hybridized carbon atoms. These two extremes provide us a lower and an upper bound for the expected C-C bond length in the cations.

ACETYLENE

The structure of acetylene was fully optimized as described in the Optimization Techniques section.

ETHYLENE

We optimized the ethylene geometry as described in the Optimization Techniques section. The only constraint placed on the system was the assumption that all found hydrogens were equivalent. Each remaining parameter was fully tested. The methylene hydrogens were even bent out of the plance of the molecule which while it was not expected to provide a best geometry served the purpose of providing a fully unrestricted optimization.

ETHANE

The ethane molecule was also fully optimized. Local C_{3v} symmetry was assumed for the methyl groups. All bond angles and bond lengths were varied until the best structure was obtained.

RESULTS

The geometric parameters for acetylene are listed in table 3 and figure 1. The geometry calculated for ehtylene is summarized in table 4. Its structure is given in figure 2. The results for ethane are summarized in table 5 and figure 3.

	Bond Lengths (Å)		Bond Angle (Degrees)	
Method	CC	CH	∠HCC	
INDO	1.200	1.100	180.0	
Experiment[a]	1.209	1.057	180.0	

a. See ref. 55

Table 3. INDO Optimized Acetylene Geometry.

Method	CC (A)	CH (A)	∠HCC (Degrees)
INDO	1.31	1.115	124.3
Experimental[a]	1.337	1.086	121.3

a.) Ref. 50

Table 4. Optimized Ethylene INDO and Experimental Geometry

METHOD	CC (A)	CH (A)	∠ HCH
INDO	1.49	1.125	109
Experimental[a]	1.53	1.093	109°45'

a.) Ref. 50

Table 5. Ethane INDO and Experimental Geometry

SPECIES	INDO[a]	INDO[b]	NDDO[c]	EXPERIMENTAL
$H_2C=CH_2$	1.31	1.31	1.367	1.337
H_3C-CH_3	1.49	1.46	1.515	1.534

a.) This work

b.) Ref. 9

c.) Ref. 13

d.) Ref. 50

Table 6. Comparison of CC bond lengths (A°)

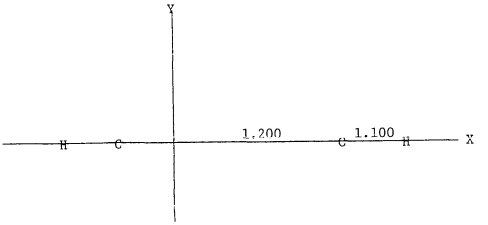

Figure 1. INDO Optimized Acetylene Geometry

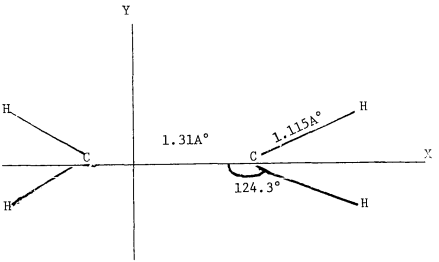

Figure 2. INDO Optimized Ethylene

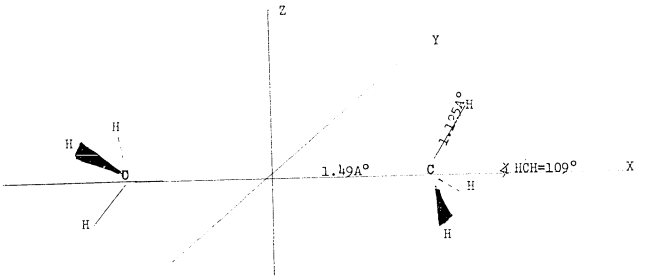

Figure 3. INDO Optimized Ethane

DISCUSSION

INDO geometries compare quite well with experiment. Ethylene is predicted to be planar with HCH angle less than 120° (see table 4 and figure 2). Gordon and Pople found that INDO reproduced geometric parameters well in a much broader study.[9,28a,28f]

The CC bonds in ethane, ethylene, and acetylene underestimated as in true in general for CNDO and INDO calculations.[28a]

PROTONATION OF ETHYLENE

Before considering the ethyl cation we treated possible pathways which would produce the cation, viz. the protonation of ethylene. The addition of a proton to ethylene to form a "π-complex" has often been proposed as an intermediate in additions of HX to olefins.[51 52] We wished to study the possible paths proton could follow during protonation. Ethylene was positioned as pictured in figures 2 and 4.

A proton was moved from an infinite distance (10A) from the origin of the axes (figure 4) to the origin along three separate paths: (1) along the z axis, (2) along the y axis, and (3) along the x axis.

Throughout protonation the ethylene moiety was assumed to be unperturbed, i.e. its geometry remained fixed at the optimum values for ethylene in figure 2.

This is, of course, an oversimplification but if there is a large energy difference between pathways the results should suggest which direction of approach is favored. (Optimization of the minimum energy structures for the z and x axis approaches will lead to optimized bridged and open ethyl cations respectively.)

We also calculated a potential surface for protonation of ethylene.

For the surface the ethylene geometry was not varied, i.e. remained the same as in figure 2, as the proton was moved in the field of this "core". The surface was generated by calculating energy points for each variation of 0.1A as x varied from 0, i.e. from the center of the cc bond, to 2.5A and as z varied from 0 to 2.5A°. The surface was thus calculated from almost 700 grid points. Contours were drawn connecting points of equal energy, see figure 5.

The optimum pathway for approach in our[15] and a recent ab initio[49a] result was along the z-axis. This path is parallel to the axis of the two $2p_z$ orbitals of carbon in ethylene. The lowest energy point for the proton on the z-axis is 1.1A° above the center of the cc bond. It is symmetrically situated 1.28A° from each carbon.

The pathway with the highest minimum energy point in both our and the ab initio work is along the y-axis. The minimum energy point is 105 Kcal/mole higher in energy in our[15] and 96 in lehn and Wipff's study than the z-axis minimum.[49a] (this energy difference in undoubtedly much larger than it would be had the geometry of the ethylene fragment been allowed to vary.) The lowest energy point is located on the y-axis 1.1A° from the center of the cc bond. It is 1.28A° from both carbon atoms.

We also considered an approach directly toward the methylene group along the x-axis. The optimum location for the proton is 1.9A° from the center of the cc bond, 1.25A° from the nearest carbon atom. The minimum along this path is less favorable than z-axis approach and the path is also less favorable because a 90Kcal/mole barrier must be surmounted. The curve for the x-axis approach becomes discontinuous as the proton approaches the methylene carbon where the repulsive energy becomes very large.

An additional approach considered by Lehn and Wipff[49a] was along the path B, figure 4, parallel to the z-axis directly onto the $2p_2$ (π) orbital of one

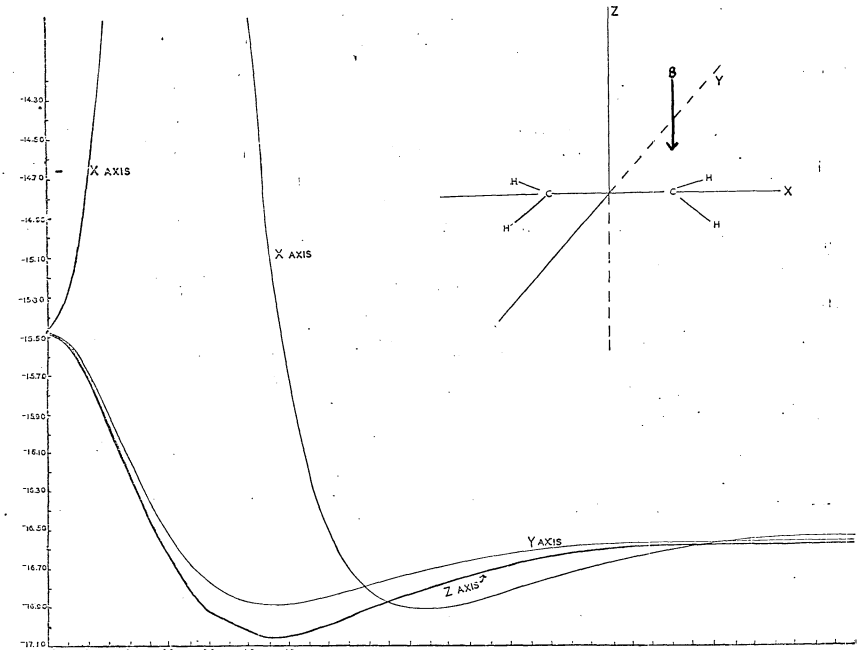

Figure 4. Plot of energy (atomic units) vs. proton approach along the axes.

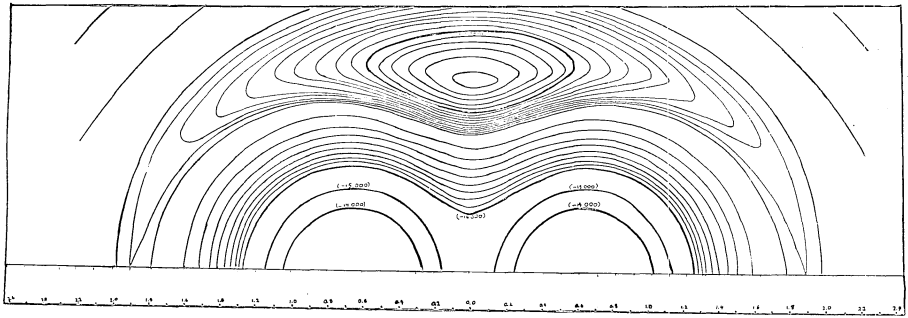

Figure 5. Potential energy surfaces for protonated ethylene. (C-C = 1.31A°)

Pathway	Z[a]	Y[a]	X[a]
ΔE^b	0	105	90
r(oH)[c]	1.1[d]	1.1[d]	1.9[e]

a.) For definition of pathways see figure 3.

b.) Energy relative to the lowest energy, Z, pathway (Kcal/mole)

c.) Distance from origin to optimum H position along indicated axis (A°)

d.) 1.28A° from both carbons

e.) 1.25A° from nearest carbon

Table 7. Relative INDO stabilities and H^+ positions for protonation of ethylene for non-varying ethylene structure.

METHOD	Z^c	ΔE_z^d	B^c	ΔE_b^d	Y^c	ΔE_y^d	X^c	ΔE_x^d
INDO[a]	1.1	0	--	--	1.1	105	1.25	90
ab initio	1.24	0	1.22	6	1.22	96	--	--

a.) Ref. 15

b.) Ref. 49a

c.) Distance (Å) from optimum H^+ position along each pathway to: (1) nearest carbon, or (2) center of cc bond (see figure 3 for definition of paths)

d.) ΔE_m difference in energy (Kcal|mole) between lowest energy path (Z) and path M (M = Z, B, Y, X)

Table 8. Relative stabilities and H^+ positions for protonation of ethylene for a non-varying ethylene structure.

carbon. It was found to be 6 Kcal/mole higher in energy than the z-axis approach.

Our potential surface for the protonation of ethylene indicates that if a proton approaches ethylene along any path the proton will spontaneously and without activation energy revert to a bridging position. The optimum position being at the z-axis approach minimum.

Lehn and Wipff[49a] indicate the open structure to be favored after optimization and suggest an initial approach along z, figure 4, until the proton begins to interact with the ethylene fragment. At this point the systems "deforms" from the ethylene structure toward the open ethyl cation configuration and the proton veers toward path B, figure 4, toward the open cation configuration. Dixon and Lipscomb[49d] indicate that their ab initio calculation suggest that interactions between the proton and ethylene begins at 3.7A° with no significant variation in ethylene cc bond length until the proton is 1.6A above the center of this bond. Their optimization studies determine the open structure to be favored by 12 Kcal/mole over the bridged structure.

DISCUSSION

The addition of H^+ to ethylene to form a "π-complex"[52] has often been proposed as an intermediate in additions of HX to olefins.[51] With the ethylene "core" positioned as in figure 4 we calculated the energies for such a protonation of ethylene along the three coordinate axis allowing for no perturbation of the ethylene geometry.

As one might expect, the favored direction of approach is along the z-axis parallel to the carbon $2p_z$ orbitals involved in the π-bond. This allows for maximum interaction and strongest bonding. Further, the potential surface, figure 5, indicates that any other path the proton

chooses will result in a spontaneous shift without activation energy to this bridged structure. While ab initio results of Lehn and Wipff[49a] do agree that the z-axis approach is the favored route, they disagree that the final structure is bridged. Dixon and Lipscomb[49d] have performed an extensive ab initio study using only a minimal basis set on protonation of ethylene along the z-axis pathway. They determine that the open ethyl cation should be the optimum structure. They warned that their conclusions might not be conclusive due to basis set limitations and correlations errors. (Pople, et.al. have shown that expansion of the basis set to include polarization functions (p orbitals on H and d orbitals on c) stabilize the bridged structures more than open.[36,38] Zurawski, et.al. have studied correlation effects and have noted that when corrections are made for correlation the bridge structure gains in energy with respect to their straight chain isomers.[40] Both studies indicate the bridged ethyl cation becomes favored over the open when these corrections are applied.)

Clark and Lilley[49b] optimized the bridged and open cations using a minimal basis set ab initio scheme. They recalculated the energies of these optimum structures adding p-orbitals functions for H to the basis set. Their conclusion that the bridged cation would spontaneously collapse to the open without activation energy was based on these energy values. To study this pathway they moved the proton directly from the bridged position to its locale in the open cation. Pople, et.al indicate that while inclusion of p-orbitals on hydrogen certainly helps improve the quality of ab initio calculations for the ethyl cation and other cases it doesn't help as much as added d-orbital function and not as much as inclusion of both.[38] This coupled with correlation errors leaves Clark and Lilley's relative energies of open vs. bridged ethyl cation of 3.39 Kcal/mole[49b] open to question.

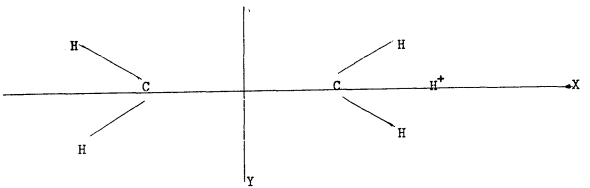

Figure 6. Protonated ethylene with proton at x-axis minimum.

The minima along the y- and z-axis position the proton 1.28A° from each carbon atom. On the x-axis the proton is 1.25A° from the nearest carbon atom. These distances are just slightly longer than the calculated CH bond lengths for ethylene, ethane (see tables 4 and 5) and the open ethyl cation (see figure 8). The CH distance for the bridging proton in our optimized bridged ethyl cation is 1.28A° the same as the above (see figure 7).

In a "non-classical" structure[41] in which a 3-centered bond exists bond lengths should be longer than two center CH bonds since on the average only one-half of an electron pair is binding the proton to each carbon center.

The longer CH bond for the proton at its x-axis minimum compared with ethylene, ethane and the open ethyl cation, q.v., is undoubtedly a consequence of the non-optimized ethylene "core" geometry which forces the adding proton, and the methylene carbon and hydrogen atoms to all be coplanar. This results in a maximization of repulsive forces (figure 6). In the open ethyl cation, the most closely related cation which we optimized, better bond lengths and energies are obtained, as would be expected, by moving these three hydrogen atoms out of the x-y plane and closer towards the methyl configuration of ethane (vide infra).

METHOD

Based upon the evidence gleaned from the protonation of ethylene we felt the starting point for our work should be the "π-complex" model of the protonated ethylene. For this model the only constraint imposed was that the four ethylene hydrogen atoms were assumed equivalent. All remaining parameters were full varied.

The open cation was treated next. For the optimization we started

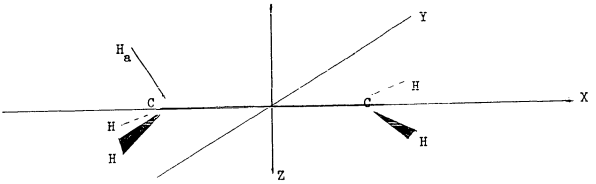

Figure 7. Initial orientation of the open, "classical" ethyl cation.

out with structure oriented as in Figure 7. The methyl group having C_{3v} symmetry and the methylene group planar, in the x-y plane. It was discovered that as H_a was moved toward a bridging position the energy became lower. There was no local minimum for an open ethyl cation. Thus, in order to optimize this cation some restriction had to be imposed on the system.

We assumed local C_{3v} symmetry for the methyl group with the same bond angles as calculated for ethane 109°. The other assumption was that the methylene hydrogens were symmetrical with respect to the x-axis. All other parameters were varied including the angle the plane containing the methylene group makes with the x-y plane.

The optimization procedure followed for these cations is described fully in the Optimization Techniques section.

If a potential surface were to be constructed for the ethyl cation one should optimize the ethylene "core" structure for each position of the proton. Since such a study is unwieldy we chose to construct a potential surface for the open structure and another for the bridged ion. This was effected for the bridged ion by plucking the bridging proton from its position in the optimized cation leaving the remaining atoms as a fixed "core". For the open cation the "core" was established by leaving all atoms except H_a (figure 7) fixed in their optimum loci.

The proton was then moved in the field of each "core" and an energy point was calculated for each 0.1Å° variation in X, or Z from X=0 to 2.5Å° and Z=0 to 2.5Å°. (Each plot was therefore constructed from almost 700 grid points). Contours were then drawn connecting points of equal energy.

Since the optimized cc bond length varied by only 0.1Å° from the bridged to the open cation the contour surfaces were combined by: (1)

superimposing the methyl carbon in the open ethyl cation with one of the carbon atoms of the bridged structure, (2) comparing calculated energies point by point choosing the lower energy value for each point to form a new "combined" surface.

RESULTS

The geometric parameters for the optimized ethyl cations are summarized in table 9; charge densities are listed in table 10. Figures 8 and 9 picture the optimum structures and charges for the "non-classical"[41] and the open ions respectively.

Our calculations demonstrate the "non-classical" ethyl cation to be 46 Kcal/mole more stable than the classical cation. In the open cation the methylene group is planar while in the bridged the methylene hydrogens are below the x-y plane.

The results of a number of reported ethyl cation studies are summarized in table 11.

The semiempirical methods favor the bridged structure. The more sophisticated ab initio results also favor the "non-classical" cation. The minimal basis set ab initio calculations favor the open cation.

Our study indicates that a proton approaching ethylene from any direction will be deflected toward a bridging position spontaneously without requiring additional energy of activation. This can be seen in our potential surfaces, figures 10,11 and 12. In the surface for the bridged as well as the open cation the energy minimum finds the proton in a bridging position. In the open cation surface and the combined surface the proton is energetically more stable in the vicinity of the methylene group than indicated in the surface for the bridged ion. No local minimum appears in any surface for the open cation. Thus the 46 Kcal/mole energy difference is dependent upon how we chose to restrict

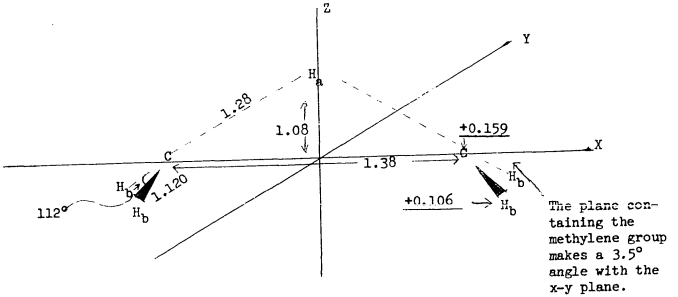

Figure 8. Bridged ("Non-classical") ethyl cation. (Charges underlined.)

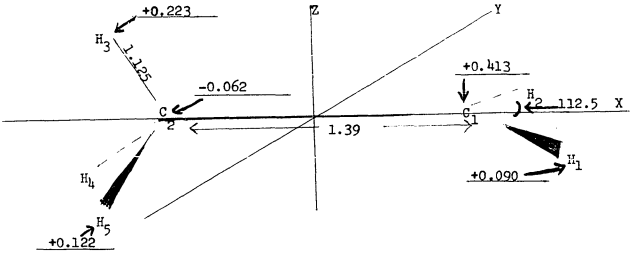

Figure 9. Open ("Classical") ethyl cation. (Charges underlined.)

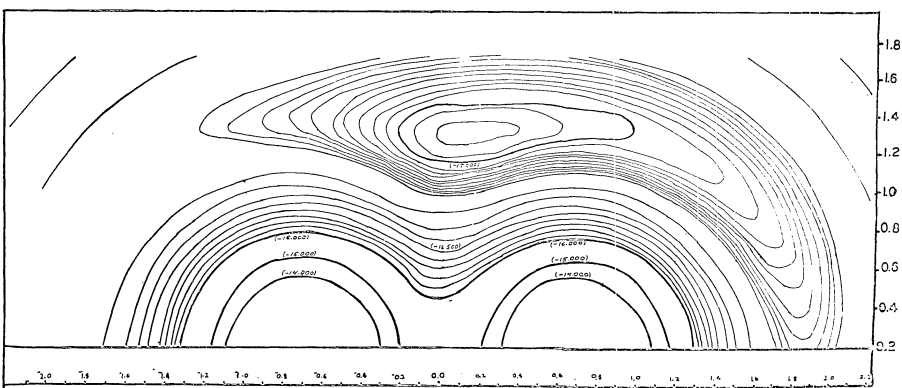

Figure 10. Potential energy surface for the open ethyl cation II.

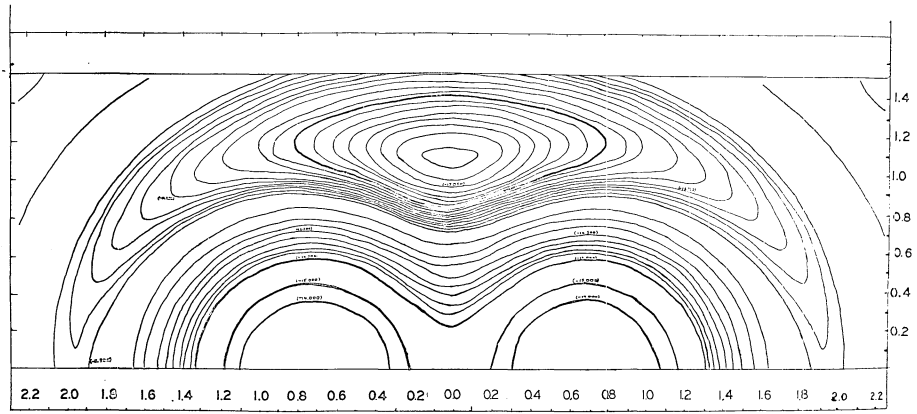

Figure 11. Potential energy surface for the bridged cation III (C-C = 1.38A°)

	BOND LENGTHS (ANGSTROMS)				ANGLES (DEGREES)		
ETHYL CATION	CC	METHYL CH	METHYLENE CH	BRIDGING CH	METHYL HCH	METHYLENE HCH	METHYLENE WITH x-y PLANE
BRIDGED	1.38	--	1.120	1.28	--	112	3.5
OPEN	1.39	1.125[a]	1.120	--	109[a]	112.5	0.0

a.) Assumed

Table 9. INDO geometric parameters for the ethyl cations, $C_2H_5^+$

ETHYL CATION	METHYLENE C	METHYL C	METHYLENE H	H_3	H_4, H_5	H_a
BRIDGED	0.159	--	0.106	--	--	0.256
OPEN	0.413	-0.062	0.090	0.223	0.122	--

Table. 10. INDO atomic charge densities for the ethyl cations.

AUTHORS	REF.	METHOD	FAVORED CATION	ΔE^{a}(Kcal/mole)
Dannenberg and Berke	15	INDO	Bridged	46
Kollmar and Smith	4	CNDO[b]	Bridged	10
Sustmann, et.al.	13	NDDO	Bridged	33[c]
Hoffmann	3	EHT	Open	2.0[c]
Sustmann, et.al.	13	ab initio	Open	9[c]
Williams, et.al.	54	ab initio	Open	11.4
Dixon and Lipscomb	49d	ab initio	Open	12
Clark and Lilley	49a	ab initio[d]	Open	5.16, 3.39[d]
Hariharan, et.al.	38	ab initio[d,e]	Bridged	0.9[d,e]
Zurawski, et.al.	40	ab initio[f]	Bridged	9[f]

a.) Energy difference between favored and higher energy cation

b.) Modified as in Ref. 53

c.) Limited geometric optimization

d.) p-functions on hydrogen included in basis set.

e.) d-functions on carbon included in basis set

f.) Correlation corrections included

Table 11. Summary of data for several ethyl cation studies.

the geometry for this system.

In the study of the bridged cation as the proton approaches the double bond the methylene protons are repelled and are pushed below the x-y plane. The deformation that occurs is consistent with a shift from sp^2 hybridization in ethylene toward sp^3 hybridization of the methylene carbon which is participating in a three-center bond in addition to having its original bonds to carbon and the original methylene hydrogens.

DISCUSSION

Our results support the formation of a π-complex during the protonation of olefins. This mechanism is frequently invoked to account for trans additions at the double bond center.[51]

Liquid phase studies have variously proposed the open or bridged ions as intermediates in the papers mentioned in the introduction to the chapter. Roberts and Yancey[43] discovered little evidence for bridging in the deamination of C^{14} labeled ethylamine, whereas Myhre and Evans[44] found a great deal of evidence for a "non-classical" intermediate either of a bridged, III, or rapidly equilibrating pair of degenerate open cations, such as II (C^{14}), and IV, in a trifluoroacetolysis of 1,1,dideuteroethyl tosylate. In this lab conclusive evidence for a bridged 2-butyl cation participation, V, in the trifluoracetolysis of 1,1,1,2-tetradeutero-VI, and 3,3,4,4,4-pentadeutero-2-butyl tosylate was found.[47]

A recent article by Schadt and Schleyer concludes that a solvent of low nucleophilicity and high ionizing power would favor neighbor participation, a bridged intermediate, over solvent-assisted pathways for the solvolysis of 2-arylethyl tosylate.[25]

A solvent can act to delocalize a developed or developing positive charge in cations and can thereby stabilize the classical carbonium

ion (with its localized positive center) more than the bridged structure. In a non-solvated environment, e.g. vapor phase, charge delocalization cannot be accomplished by the solvent but can occur through a three-centered σ-framework. Thus a "non-classical" structure should become more favorable in such an environment. The medium one chooses to run experiments in may thus have a large effect on the outcome of experiments. This suggests that since theoretical data do not take solvation into account application of calculated results must be applied to solvated systems with due caution.

Recently gas phase studies have been appearing at enormous rates.[21-23] As noted earlier an ion cyclotron resonance study of the decomposition of diethyl-N-nitrosomine by Jaffé and Billets[21c,d] suggests that either a non-equilibrated bridged or open ethyl cation is involved in the decomposition. A mass spectral study by Ausloos, et. al.[23c] indicated that the barrier to hydride shift in the ethyl cation must be less than 5 Kcal/mole. Results of this work can be interpreted as suggesting that either a bridged, or rapidly equilibrating degenerate pair of cations may participate in the decomposition of the deuterated ethyl iodides and bromides tested. Thus solution as well as gas phase data do not clearly establish whether the classical or "non-classical" cation is energetically more stable.

The position chosen for the location of the bridging proton in the open ethyl cation affected the energy barrier between the open and bridged cation. Since no local minimum existed for the open structure the choice was arbitrary. As mentioned above, the closer the proton approached a bridging position the better the energy was (see figure 10). Thus if we were to place the proton in the open structure closer to the bridging position our energy barrier would decrease significantly toward the mass spectrally determined limit of 5 Kcal/mole.[23c]

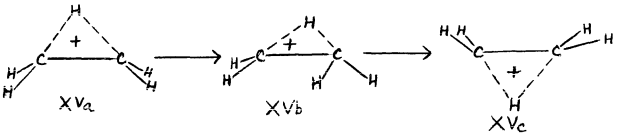

Hydride migration can occur through the sequence XVa→XVb→XVc with little displacement of hydrogen from its bridging position. Figure 10 indicates that such a pathway would be much closer to the 5 Kcal/mole barrier than the difference between the open cation configuration we chose and the bridged cation.

For all of the other studies of the ethyl cation system this same problem must have arisen, viz. a geometry had to be assumed for the structure exhibiting no local minimum. (If the studies produced a local minimum for both II and III this difficulty is obviated.) The very nature of the geometric choice determines the calculated magnitude of the barrier.

Results of theoretical studies seem to be no more conclusive (see table 11). The CNDO method was shown to have a bias toward three-member ring strucutres by Snyder[33] (table 1). Presumably INDO also shows the same bias. This may be a consequence of neglecting three- and four-center electron repulsion integrals. The stability of the bridged structure is therefore overestimated in the studies by Dannenberg and Berke,[15] and Kollmar and Smith.[4]

The NDDO study by Sustmann, et. al.[13] agrees quantitatively with our conclusion. They assumed that the four equivalent hydrogen atoms in the bridged structure were planar. To test the effect of this approxima-

tion on the calculated energy of III we determined the energy of our optimized bridged cation using the INDO approximation with these four hydrogens forced into the xy-plane. This configuration was found to be 10 Kcal/mole less stable. This correction if approximately the same for both the INDO and NDDO treatments when applied to their study brings the NDDO energy difference between cations II and III into close agreement with ours. If the bias of the CNDO method is due to neglect of three- and four-center electron repulsion integrals then NDDO will also overestimate the stability of 3-member ring structures. The NDDO approximation has not been widely tested and the quality of its results not determined.

Sustmann, et.al.[13] used the same geometric assumption as in their NDDO in their ab initio study of the ethyl cation system. This forcing of the ethylene "core" to be planar will cause the energy of their bridged structure to be too high. The energy difference between the ions II and III will become close to zero if the correction in energy due to the constraint is approximately the same as calculated by the INDO method.

In addition as with all minimal basis ab initio calculations, the bridged cation gains in relative stability with respect to the open isomer as polarization functions (p orbitals for H, and d-functions for C) are added to the basis set.[38] Inclusion of d-functions for the ethyl, vinyl and methyl cations produced greater stabilization than p-orbitals.

Thus in the studies by Sustmann, et.al.[13], and Williams, et.al.[15] and Dixon and Lipscomb [49d]in which polarization functions were included they all concluded that the open structure was favored. With expansion of the basis sets to include polarization functions the energy difference will be lowered. This is seen, for instance, in the study by Clark and Lilley[49a] who include p- but not d-functions. Hariharan, et.al.[38] found that with a basis set including both p- and d-functions the bridged ethyl

cation was the favored one. In this paper they predict that the bridged structure may well be the optimum isomer in the Hartree-Fock limit.

In a study of the effects of electron correlation on the relative stability of the ethyl cations Zurawski, et. al.[49] concluded that omission of electron correlation favors the open cation. The bridged structure is thus further stabilized as correction for correlation effects are added. In this paper the inclusion of correlation corrections produced a bridged ethyl cation which was more stable than the open ion.

In extending our application of the INDO method[3] to other organic cationic systems we next selected the sec-butyl carbonium ion. It is the simplest secondary carbocation capable of symmetrical hydrogen bridging. In addition, due to its greater intrinsic stability as compared with the primary ethyl cation we felt that we could perform a solution-phase study of the viability of a bridged 2-butyl cation.[47] These results could provide support for the INDO results.

While correlation would not necessarily be expected between solution-phase and theoretical results, unless solvation were constant along the reaction pathway, or constant for the structures being compared, theoretical data can be suggestive of phenomena for which to watch.

In our INDO study of the 2-butyl cation, we sought to study the relative stabilities of the classical, and bridged (tetra-coordinated[56]) cations. The information we would obtain from experimental work may not necessarily imply their relative stabilities because the degree of participation of a bridged or open cation can be influenced by choice of reaction conditions.[25] The barrier to interconversion of the open and bridged cations is thought to be about the same magnitude as the barrier which must be surmounted to produce solvolysis products.[57]

J. D. Roberts and coworkers[58] obtained only 9% rearranged 2-butyl-4-C^{14} acetate on acetolysis of 2-butyl-1-C^{14} tosylate under conditions which almost totally eliminate any bimolecular (Sn2) reaction. A "non-classical" carbonium ion XVI, or a rapidly equilibrating pair of open cations, XVIIa and b, cannot participate to more than 18%, or 9% respectively.

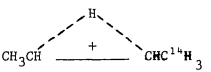

XVI

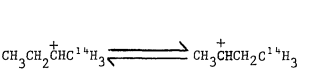

XVIIa XVIIb

Saunders, et. al.[59] studied proton NMR spectrum of the 2-butyl cation in "magic acid"[60] (FSO_3H - SbF_5) at -110°C. He only noticed two resonances indicating a rapid equilibrium between degenerate cations of the form of XVIIa and b. They suggest a barrier to the 2,3-hydride shift to be less than 6 Kcal/mole and an interconversion rate in excess of 200,000 sec^{-1} at -112°C.

Proton NMR studies of the sec-butyl cation in SO_2ClF - SbF_5 at -120°C give two peaks of relative area 2:1. This was interpreted by Olah and White, based upon predicted chemical shift and C^{13}-H coupling constant to indicate that the cation exists as rapidly equilibrating pair of degenerate ions, XVIIa and b. Their arguments are somewhat tenuous since the two central carbons in the model they used for the bridged sec-butyl cation, XVI, was assumed to be in a hybrid state somewhere between sp^2 and sp^3.[61] Our INDO results show that these carbons are sp^2 hybridized (vide infra). The increased s-character afforded by the sp^2 hybridization would result in greater shielding for C_2 and C_3 than in Olah and White's model. A rapid equilibrium between bridged 2-butyl cations, XVIIIa-c, would also explain the appearance of two resonance and a relative peak area of 2:1. (Strother's book Carbon-13 NMR Spectroscopy[62] provides a good review of the field.)

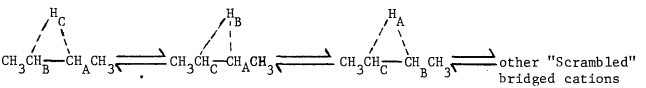

XVIIIa XVIIIb XVIIIc

The work done in this lab,[47] discussed in the ethyl cation section, on the trifluoroacetolysis of deuterated 2-butyl tosylates clearly establishes significant participation of a bridged butyl cation XVI. Schadt and Schleyer[25] found that trifluoroacetic acid strongly favors aryl-assisted over solvent assisted pathways for the solvolysis to 2-arylethyl tosylates.

Theoretical results for bridged and open cations were discussed extensively in the ethyl cation section (q.v.). They were no more conclusive than the above as to whether the open or bridged carbonium ions are more stable. No theoretical studies have been reported for the 2-butyl cation system.

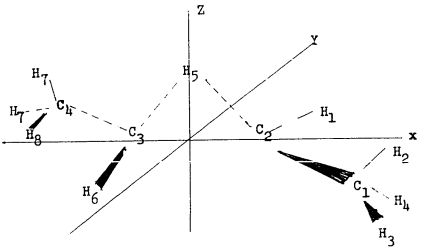

XIX

Figure 13. Unoptimized bridged 2-butyl cation.

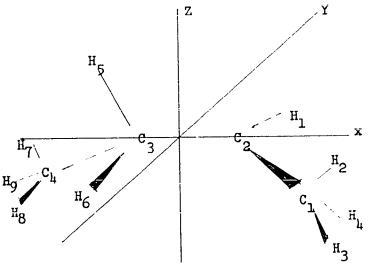

XX

Figure 14 **Unoptimized open 2-butyl cation.**

Our INDO level study of the sec-butyl cation is described in detail below.

METHOD

For both ions the bridged (XIX, fig. 13) and the open (XX, fig. 14) the C_2C_3 bond was set along the x-axis with the z-axis as perpendicular bisector of the bond.

The only constraints placed on the bridged isomer were: (1) the position of one methyl group could be determined from the coordinates of the other by a 180° roatation around the z-axis, i.e. by multiplying the x and y coordinates by -1. (2) In a similar fashion the coordinates of H_6 could be obtained from H_5 by a rotation of 180° around the z-axis. (The molecule thus is assumed to possess C_{2v} symmetry.) (3) The methyl groups were assumed to have the same bond angles (109°) and lengths (1.125Å) as in ethane, i.e. they possess local C_{3v} symmetry. All other parameters were fully optimized.

While optimizing the open sec-butyl cation the same difficulty arose as with the ethyl cation (q.v.),viz. no local minimum could be obtained for such a species. Optimization was pursued with H_5 in approximately the same position in the x-z plane as the methyl hydrogen in ethane. The only other constraint placed on the system was that each methyl group possessed the same geometry as in ethane, i.e. local C_{3v} symmetry with bond angles of 109° and CH distances of 1.125A. Each remaining parameter was fully optimized as it was for the bridged cation.

The optimization procedure is described in detail in the "Optimization Techniques" section.

To generate a potential surface for the 2-butyl cation a geometric optimization should be effected for the "2-butene core" for each position of the proton. Since such a study is unwieldy we decided to determine one potential surface for the open cation and a second for the bridged. The bridged surface should best describe the motion of the proton in the region between carbons 2 and 3 while the open cation surface should best describe the motion of the proton near C_2 or C_3 as was found with the ethyl cation. To generate the surfaces H_5 was removed from each optimized structure, see figures 13 and 14, and the remaining fragments were used as fixed "cores".

The proton was then moved in the field of each of these "cores". An energy point was calculated for every 0.1A variation in x from 0.0 to 2.5A and z from 0.0 to 2.5A. (The surfaces were thus generated from almost 700 grid points.) Contours were then drawn connecting points of equal energy.

RESULTS

The results of our optimization for the bridged, XIX, and open, XX, 2-butyl cations are summarized in tables 12, 13 and 14, and figures 15 and 16. The potential surfaces are figures 17 and 18.

The optimum bridged cation is planar with the exceptions of the bridging hydrogen and the methyl hydrogens. This is somewhat surprising in light of the evidence from the ethyl cation (q.v.) that its bridged configuration was non-planar. In contrast to the bridging proton in ethylene the positive charge is reduced by 28% (from 0.256 in the ethyl to 0.185) in the 2-butyl cation. Again, in contrast to the open ethyl

BOND LENGTHS (angstroms, A°)

2-BUTYL CATION	C_1C_2	C_2C_3	C_3C_4	C_2H_1	C_1H_2	C_3H_5	C_3H_6
Bridged,XVI	1.450	1.400	1.450	1.125	1.125[a]	1.300	1.125
Open, XVII	1.420	1.410	1.500	1.125	1.125[a]	1.130	1.125

a) Assumed

Table 12 INDO bond lengths for optimum 2-butyl cation.

2-BUTYL CATIONS	$H_1C_2C_1$	$H_2C_1H_3$	$H_5C_3{}^{Pb}$	$C_3C_6{}^{Pb}$	$H_1C_2{}^{Pb}$	$C_1C_2{}^{Pb}$	$C_4C_3{}^{Pb}$	$H_6R_3C_4$
Brdiged, XVI	114	109[a]	58	0	0	0	0	114
Open, XVII	115	109[a]	50	-10	0	0	-30	121

a.) Assumed

b.) ABP - angle between the AB bond and the x-y plane. (The sign indicates the sign of the z-coordinate.

Table 13. INDO bond angles for the 2-butyl cation.

2-BUTYL CATION	C_1	C_2	C_3	C_4	H_1	H_2	H_3	H_4	H_5	H_6	H_7	H_8	H_9
Bridged, XVI	0.008	0.184	0.184	0.008	0.060	0.064	0.042	0.061	0.185	0.060	0.064	0.042	0.061
Open, XVII	-0.039	0.359	-0.048	0.077	0.035	0.144	0.074	0.075	0.194	0.082	0.013	0.031	0.004

Table 14. INDO calculated charge densities for open and bridged 2-butyl cations.

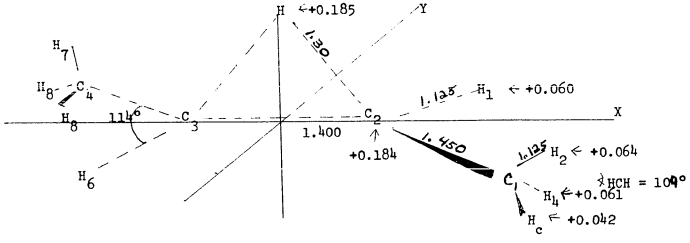

Figure 15. INDO optimized bridged 2-butyl cation.

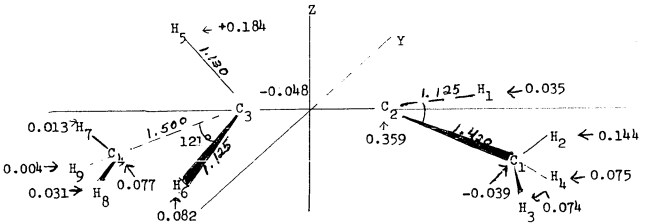

For other angles see Table **3**.

Figure 16. **INDO Optimized open** 2-butyl cation.

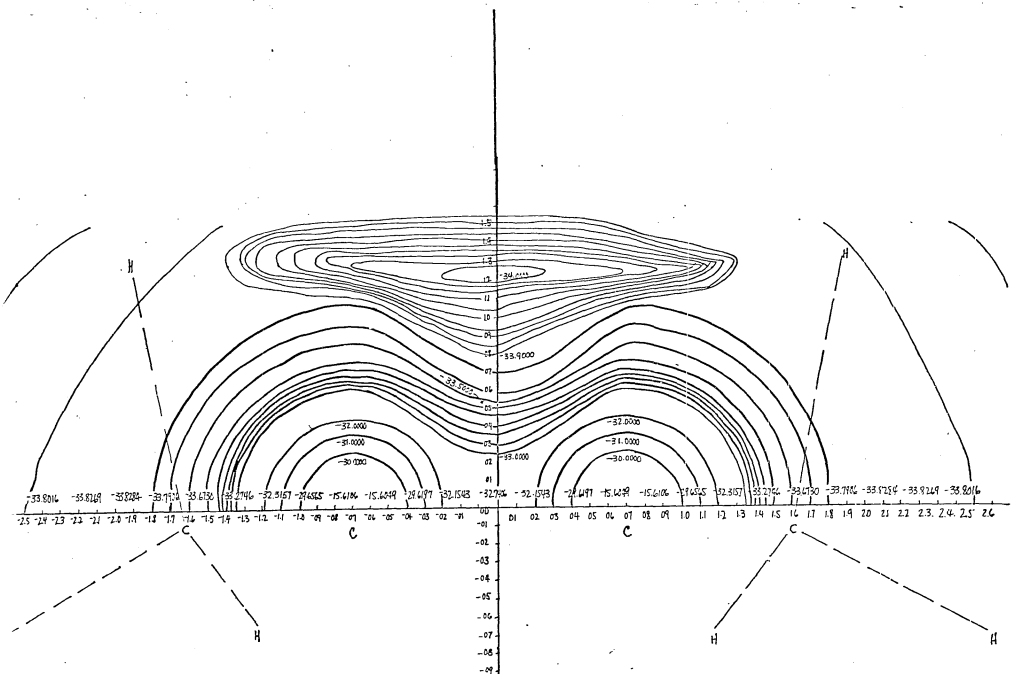

Figure 17 INDO Potential Surface for Bridged 2-butyl cation.

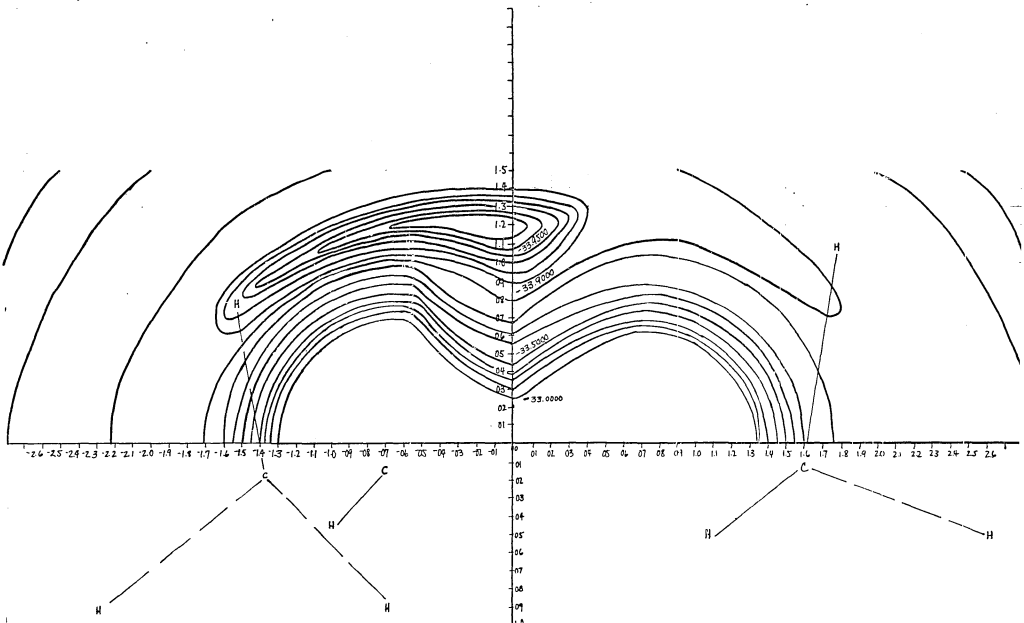

Figure 18. INDO Potential Surface for Open 2-butyl cation.

cation the cationic center in the open sec-butyl cation shows a lesser positive charge. We have found the bridged cation to be 46 Kcal/moles more stable than the open. Further, a look at either potential surfaces indicates that protons which initially add to form an open structure will spontaneously collapse to a bridging position without activation energy. The surface for the open cation indicates that the proton will be energetically more comfortable in the vicinity of C_2 or C_3 than is indicated by the surface for the bridged cation.

DISCUSSION

In our ethyl cation[15] work the protonation study indicated and optimization confirmed that the preferred mode of additions is via a "π-complex"[52] mechanism. The potential surfaces (figures 17 and 18) further emphasize this by indicating no minimum other than the one for a proton in a briding position. This suggests that if a proton were to add from any pathway other than the one leading to "π- complex" formation it would spontaneously and without activation energy collapse to the "π- complex". This is in accord with current theories for protonation of alkenes.[51]

While there is a growing general feeling that the bridged cation is probably the more stable one in the Hartree-Fock limit[38,40,49d] our energy difference is undoubtedly exaggerated. Snyder demonstrated that the CNDO, and thus presumably the INDO, method is biased toward 3-member ring structures.[33] This combined with the restrictions imposed on the proton, H_5, in the open cation certainly causes the bridged cation to be exaggeratedly favored.

It was noted that the positive charge on the open 2-butyl cation center is lesser than that on the open ethyl cation. In a population analysis the $2p_z$ orbital of the sp^2 carbon increases in electron density from

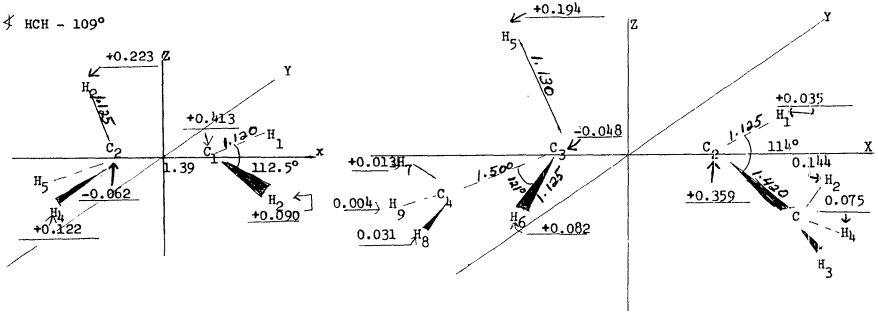

Figure 19. Optimized geometries for the open ethyl and 2-butyl cations. Charges are underlined.

0.315 in the ethyl to 0.489 in the 2-butyl cation. This is accompanied by a net loss of σ-electron density of 0.120 on this carbon. A similar effect caused by an α-methyl group was noted by Pople, et. al.[63b] in comparing open ethyl, 2-propyl and t-butyl cations. It led them to conclude the methyl group acts in this case as a σ-acceptor and a π-donor of electron density. They also noted an increase in bond length going from the open ethyl to the 2-propyl as we do in going from the open ethyl to the 2-butyl cation which is attributable to a decrease in double bond character as methyl groups are added.

Olah and White, based upon chemical shifts in a C^{13} NMR study, interpreted that methyl groups added α to sp^2 carbon atoms makes the carbonium carbon more positive. The noted downfield shift can alternatively be explained in terms of the above noted donor-acceptor picture of methyl groups. If methyl groups donate π-electron density and remove σ-electron density the shielding of the carbonium carbon will decrease. The same downfield shift will result with little, if any, change in charge on the sp^2 carbon.

We also found direct evidence for a hyperconjugative effect in the "non-classical" 2-butyl cation.[64] A comparison of the bridged ethyl cation and the bridged 2-butyl cation, figure 20, indicates the contribution of hyperconjugation to the stability of the 2-butyl cation. In the ethyl cation the four H_a's are not coplanar with the two carbon atoms (they are bent 3.5° below the plane.) In the case of the 2-butyl cation, however, H_1 and H_6 are coplanar with the four carbons. If one considers the bridged ethyl cation as arising from the protonation of an ethylene molecule, one would expect the H_a's to move out of the ethylene plane in the direction opposite from the incoming proton. (This has been discussed above in great detail, and is exactly what is found.) Such a distortion would be expected from the increasing sp^3 character of the carbon orbitals

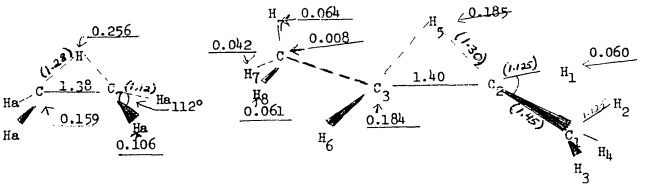

Figure 20. Optimized geometries for the bridged ethyl cand 2-butyl cations. Charge densities are underlined, bond lengths are in parenthesis. For the ethyl cation the CH_a bonds make an angle of 3.5° with the plane containing the two carbon atoms and perpendicular to the 3-member ring. For the 2-butyl cation all four carbon atoms and H_1 and H_6 are coplanar.

in the CH_a bonds and from the tendency to minimize the repulsion between the bridged proton and the H_a's.

In principle one should expect an analogous distortion from planarity if one considers the protonation of trans-2-butene to form the bridged trans-2-butyl cation. The observation that no such distortion is predicted by the INDO calculated geometry suggests that there exists a hyperconjugative interaction between the two methyl groups and the protonated π-system. Furthermore, the maximization of this hyperconjugative interaction must contribute more to the stability of the ion than would the displacement of the two methyl carbons and H_1 and H_6 out of the plane as in the ethyl cation.

To obtain an approximate estimate of the stabilization due to hyperconjugation, the energy of an ethyl cation of the same geometry as figure 20, except that the H_a's were made coplanar with the carbon atoms, was calculated. This energy was found to be 10 Kcal/mole higher than that of the optimized structure. Reasoning that, in the absence of hyperconjugation, the bridged 2-butyl cation would have to overcome a similar barrier to keep its H_1 and H_6 in the same plane as the four carbons, the stabilization due to hyperconjugation must be $\geq$ 10 Kcal/mole.[64,65] This estimate seems in reasonable accord with the work of Baird,[66] who estimated the hyperconjugative stabilization of carbonium ions by comparing separate CNDO calculations of the same ions with the interactions of the methyl hydrogen and the adjacent carbon either included or neglected.

Further effect of hyperconjugation can be gleaned from figure 20. The 28% decrease in positive charge of the bridging hydrogen when the two methyl groups are added is caused by a transfer through space of electron density from the α-methyl group to the bridging hydrogen. This effect was noted above, for π-charge transfer to $2p_z(C^+)$ in the open 2-butyl cation when compared to the open ethyl cation. Maximization of the hyperconjugative

interaction in the bridged 2-butyl cation is observed when we rotated one of its methyl groups.

One methyl group from the optimized bridged 2-butyl cation was rotated at 5-degree intervals and the energy for each rotamer was calculated. The three-fold barrier was determined to be 5.0 Kcal/mole. The plot of a rotation from zero to 120 degrees is given in figure 21.

Figure 21 illustrates that the energy minimum corresponds to a structure with a methyl hydrogen slightly distorted (Ca. 5°) from the position eclipsing the bridged hydrogen (see figure 22) whereas the energy maximum corresponds to a structure which is more or less skew. Thus maximization of hyperconjugative interaction seems more important to the stability of the ion than does minimization of the H-H repulsions. Furthermore the minimum energy conformation has a distortion from the eclipsed geometry in the direction that maximizes the interaction of the C_1-H_2 bond (figures 20 and 21) with the π-system as it rotates this bond away from the node of the π-system. (Since H_2 is nearer the center of the π-system than is H_3, a rotation in this direction should be more beneficial than a rotation in the opposite direction.)

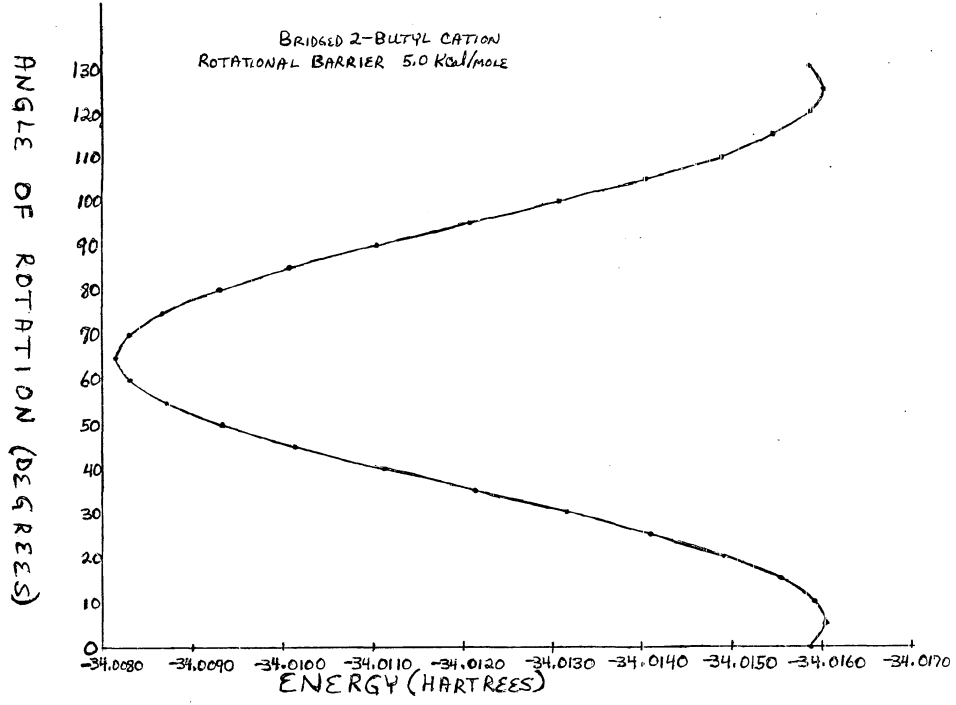

Figure 21. Barrier to Rotation of a Methyl Group in 2-butyl cation.

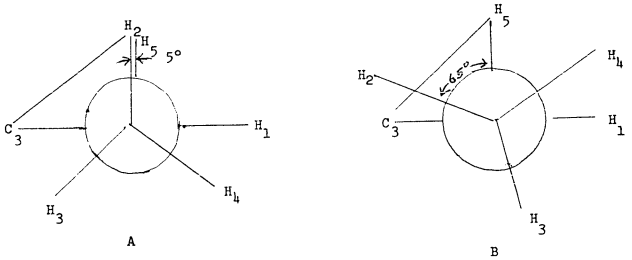

Figure 22. Rotation of a methyl group in the bridged 2-butyl cation. (A) minimum energy and (B) maximum energy configurations.

The phenonium ion, XXI, has been the focus of many current as well as part research efforts. This includes much experimental as well as theoretical work. Cram proposed the existance of the phenonium ion, XXI as an intermediate in the acetolysis of the optically active L-erythro, XXII, and L-threo, XXIII, 3-phenyl-2-butyl tosylates (figure 23).

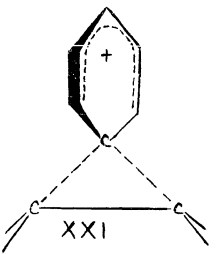

XXI

Acetolysis of the L-erythro tosylate, XXII produced only the L-erythro acetate, XXIV. Acetolysis of the L-threo tosylate, XXV, yielded a racemic mixture of the D-, XXVII and L-threo, XXVIII acetates.

Cram argued that these results indicated participation of a phenonium ion as an intermediate for both tosylates. In the acetolysis of the L-threo tosylate, the product formed depended upon whether the acetate attacked C_α or C_β in the symmetric bridged intermediate, XXVI. In the former case, attack at either carbon of the asymmetric XXIII would yield exclusively XXIV.

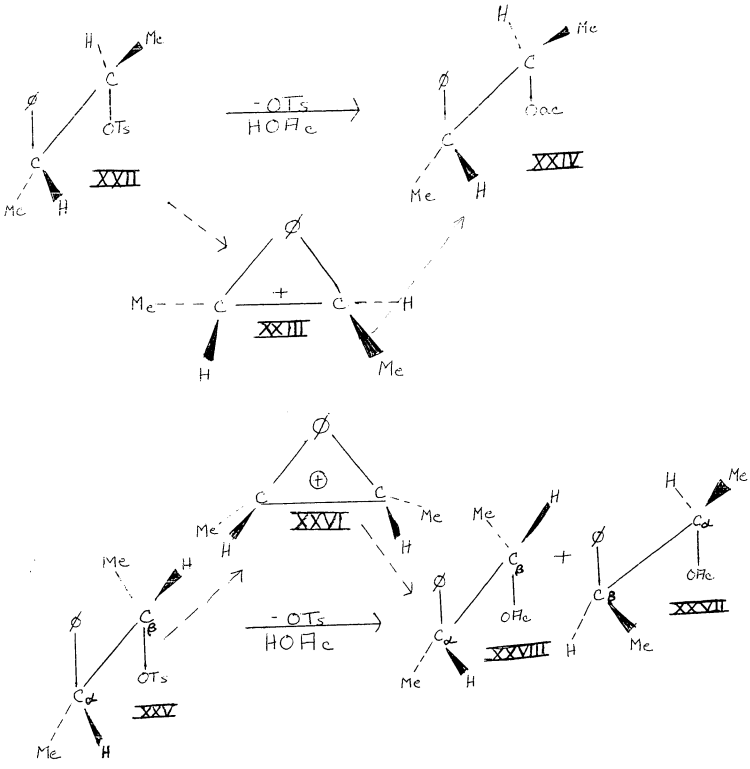

Figure 23. Acetolysis of L-erythro, XXII, and L-threo, XXV, 3-phenyl-2-butyl tosylates.[68]

Cram also determined that the presence of the phenyl group in threo-β-phenyl-2-butyl tosylate should enhance the acetolysis rate 24 times as compared with 2-butyl tosylate. This argument was based upon two factors: (1) threo-3-phenyl-2-butyl tosylate undergoes ionization three times as rapidly as 2-butyl tosylate,[68] (2) the predicted effect of phenyl substituents is to decrease rates of acetolysis by a factor of eight.[68] Since this rate retardation is not observed, threo-3-phenyl-2-butyl tosylate undergoes acetolysis eight times more rapidly than predicted. The factor 24 indicates phenyl participation in ionization of 96% for threo-3-phenyl-2-butyl tosylate in good agreement with a 99% figure from product and stereochemical data.[68,69]

The interpretation of these results was questioned by Brown who argued that the pathway does not require the presence of a "non-classical"[41] cation. Instead he proposed a rapid equilibrium between classical degenerate isomeric forms, XXIXa and XXIXb, which is more rapid than the rate of rotation around the C_α-C_β bond[70,71] to explain the experimental results.

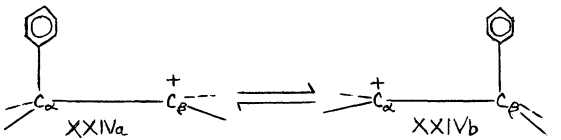

XXIVa XXIVb

Brown further argued against the requirement of a phenonium ion intermediate by noting that ethyl tosylate undergores acetolysis 2.7 times faster than β-phenylethyl tosylate with only 5% rearrangement. This indicates that the highly nucleophilic,[72] poorly ionizing[73] acetic acid was able to successfully compete with the phenyl group for the α-carbon.[70]

Schadt and Schleyer found that in the less nucleophilic formic acid the β-phenylethyl tosylate reacts 2.1 times as rapidly as the ethyl tosylate. Thus as competition from solvent decreases the anchimerically assisted pathyway becomes favored. The mechanism thus shifts from Sn2 in acetic acid to Sn1 in formic acid.

Nordlander and Deadman found trifluoroacetolysis of 2-phenylethyl-1,1-d_2 tosylate yielded equal quantities of the major products XXX and XXXI.[74] The rearranged products and the fact that β-phenylethyl tosylate undergoes trifluoroacetolysis 3040 times as rapidly as ethyl tosylate led them to conclude the reaction proceeds entirely through the phenonium ion.[74]

$Ph\text{-}CH_2CD_2O_2CCF_3$ XXX

$Ph\text{-}CD_2CH_2O_2CCF_3$ XXXI

For the 2-phenylethyl-1,2-d_2 brosylate system Jablonski and Snyder found that the trifluoroacetolysis occurs with total retention of configuration.[75] The same result was found by Nordlander and Kelly for 1-phenyl-2-propyl-tosylate.[76]

Olah concludes from ^1H- and ^{13}C - NMR studies that the phenylethyl cation exists as a bridged structure.[77]

Schadt and Schleyer's study of the relative rates of solvolysis of 2-phenylethyl tosylate vs. ethyl tosylate over a range of solvents has been reported earlier (vide supra).[25] They noted that with decreasing nucleophilicity and, to a lesser extent, with increasing ionizing power of the solvent the phenyl assisted pathway became dominant.[25]

This and the above studies emphasize that the participation of phenyl assisted pathway, is extremely solvent dependent. Any generalization, or comparisons of experimental with theoretical results in carbonium ion studies must be done taking, among other equally well known factors,[78] into consideration variations in solvent properties.

Since calculations should best represent gas-phase phenomena due to lack of consideration of solvent interactions, correlations of theoretical results with solution-phase data must be made with due cuation.

A solvent can act to delocalize the developed, or developing charge in cations and can thereby make the classical, open, carbonium ion more stable than the bridged structure. In a non-solvated environment, e.g. vapor phase, charge delocalization cannot be accomplished by the solvent thus a three-centered cation should become more favorable since delocalization can occur through the σ-framework. (An interesting note in this regard is the cyclopropane system. Burke and Lauterbur[79] were able to reproduce the ^{13}C NMR shielding in cyclopropane by assuming a ring current, analogous to the benzene π-system current , exists in this σ- bonded system. No theoretical basis was offered for this assumption.) Since only the molecule can be polar in a non-solvated environment it is to be expected that delocalization would be important in the gas phase.

Correlation between theoretical and solution-phase results can only be expected if solvation is constant or proportional in ions being compared. Theoretical calculations can nevertheless be suggestive of phenomena for which to watch or seek in experimental work.

Snyder performed a CNDO level theoretical study of the 2-phenylethyl to phenonium cation transofrmation.[33] His results indicate the bridged cation XXI, to be 20 Kcal/mole more stable than the open 2-phenylethyl cation, XXIX. This is in qualitative agreement with our preliminary results for this system.

Our study of the β-phenylethyl cation system began shortly before Snyder published his work.[33] The bridged, phenonium ion had been fully optimized and preliminary optimization had been done on the open cation. Our results indicate that we should expect the non-classical[41] structure to be more stable than its classical counterpart. The barrier, at this low level of optimization, was determined to be about 45 Kcal/mole which obviously should decrease substantially on optimization.

Due to similarities in results produced by the CNDO[6,7] and the INDO[8] methods[28f] it would have been little more than an academic exercise to determine the relative stabilities of XXI and XXIX. We abandoned the geometry search for the open cation for that reason. Our results for the "non-classical" structure show a number of details not considered by Snyder (vide infra).

From Snyder's results it appears that if an open phenylethyl cation were to form it would collapse without activation energy to the phenonium ion, XXI. This is exactly the stability order we have predicted for the ethyl and sec-butyl cations (q.v.) and, again, our preliminary results for the 2-phenylethyl cation indicated that this system would also present such a potential surface.

METHOD

To begin optimization of the phenonium ion, the "ethylene" portion of the ion was situated in the x-y plane. The C_7-C_8 bond was on the x-axis with the z-axis as perpendicular bisector of this bond. (see figure 24).

The benzene ring was located in the y-z plane with the z-axis running through C_1 and C_4 i.e. the z-axis bisects the benzene ring.

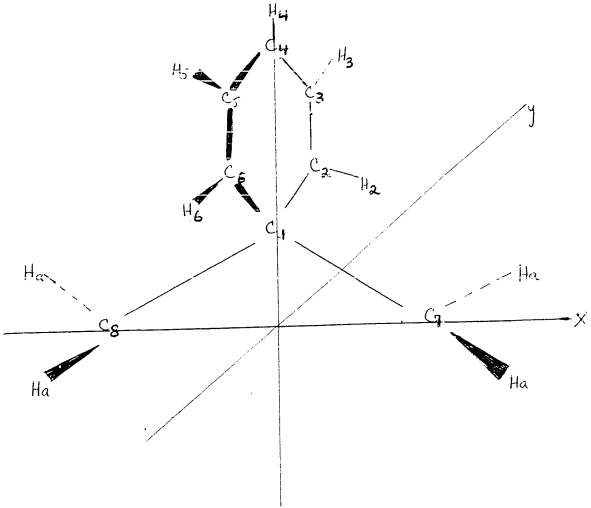

Figure 24. Non-optimized phenonium ion.

The only constraint placed upon the system was that the four ethylene hydrogen atoms, H_a, were assumed to be equivalent, and the ring was assumed to possess symmetry with respect to the C_1-C_4 internuclear axis as a C_2 axis.

All other parameters, all bond angles and bond lengths, were allowed to vary until optimization was achieved. The procedure followed to reach geometric optimization is fully described in the "Optimization Techniques" section.

RESULTS

The geometric parameters and charge densities for the phenonium ion are listed in tables 15, 16, and 17 and are summarized in figure 25.

In this ion, as in the bridged ethyl cation (q.v.), the "ethylene" hydrogens are located below the x-y plane (see also figure 26). In contrast, the two carbon and two hydrogen atoms attached to C_2 and C_3 of the 2-butyl cation are all coplanar, i.e. C_2 and C_3 are sp^2 hybridized. In addition, angles $H_aC_7H_a$ and $H_aC_8H_a$ contract to 110° and bond C_7C_8 lengthen with respect to the bridged ethyl cation (figure 26).

The benzene ring undergoes significant change from D_{6h} symmetry. The bond angle $C_2C_1C_6$ contracts to 117.6° and the C_1C_2 and C_1C_6 bonds lengthen from the expected 1.40A [28a] (an average of CC ethylene and cc ethane (=(1.31 + 1.49)/2). The entire ring geometry shifts to accommodate this change. Snyder indicates similar a lessening of the $C_2C_1C_6$ angle and lengthening of the $C_1C_2$and C_1C_6bonds.[33] His treatment restrained the remaining ring parameters so that the other changes in the ring evident in figure 25 are not considered.

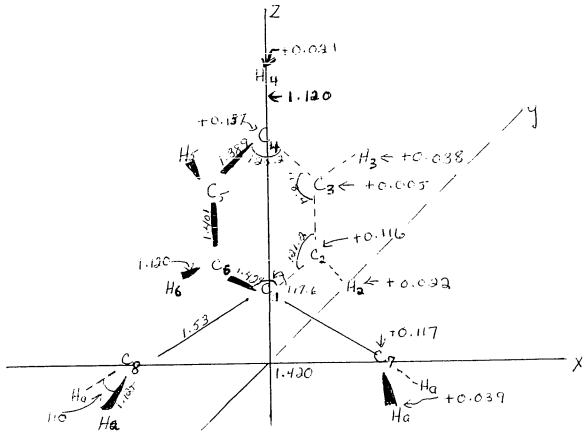

Figure 25. INDO optimized phenonium ion geometry and charge densities.

BOND LENGTHS (angstroms, A°)						
C_7C_8	C_7H_a	C_1C_6	C_1C_6	C_6C_5	C_5C_4	RING CH
1.420	1.125	1.53	1.429	1.400	1.389	1.120

Table 15. INDO optimized phenonium ion geometry. Bond lengths.

BOND ANGLES (Degrees)						
HaC_1Ha	HaC_7P^a	HaC_8P^a	$C_2C_1C_4$	$C_1C_6C_5$	$C_4C_5C_6$	$C_3C_4C_5$
110°	13°	13	117.6	128.2	118.4	123.2

a.) HaC_bP is the angle the Ha - C_b bond lies below the x-y plane.

Table 16. INDO optimized phenonium ion geometry. Bond angles.

POPULATION ANALYSIS

C_7	C_1	C_4	C_5	C_6	Ha	H_4	H_5	H_6
0.117	0.072	0.157	0.005	0.116	0.039	0.021	0.038	0.022

Table 17. INDO charge densities for the optimized phenonium ion.

Comparison of parameters with INDO optimized corner-protonated cyclopropyl cation[80] figure 27 indicates similar "ethylene" C_7C_8 and "ethylene carbon" to bridging carbon bond lengths C_1C_7 and C_1C_8. All of these cc lengths are longer than the INDO calculated cc bond in ethane (1.49A°).[15]

Table 18 indicates that the relative charge concentration in the 3-member rings decrease in the order ethyl, 2-butyl, cyclopropyl, phenonium cation.

DISCUSSION

If the phenyl cation is allowed to approach the π-system of ethylene, i.e. approach parallel to the axis of the $2p_z$ orbitals forming the π-bond, a π-complex[52] will form. It should be expected that the four hydrogens, H_a, should drop below the x-y plane to minimize repulsion. The C_7H_a and C_8H_a bonds make an angle of 13° with the plane that contains the C_7C_8 bond and is perpendicular to the 3-member ring. This indicates a change in hybridization of C_1 and C_2 from sp^2, in ethylene, toward sp^3.

This is further evidenced by contraction of the $H_aC_7H_a$ and $H_aC_8H_a$ bond angles to 110°, very close to the sp^3 bond angle, and the increase in C_7C_8 bond length to 1.420A°, both changes are with respect to ethylene. A comparison of the bridged ethyl cation and the phenonium ion also indicates similar changes, viz. a lengthening of the C_7C_8 bonds and a contraction of the $H_aC_7H_a$ and $H_aC_8H_a$ angles.

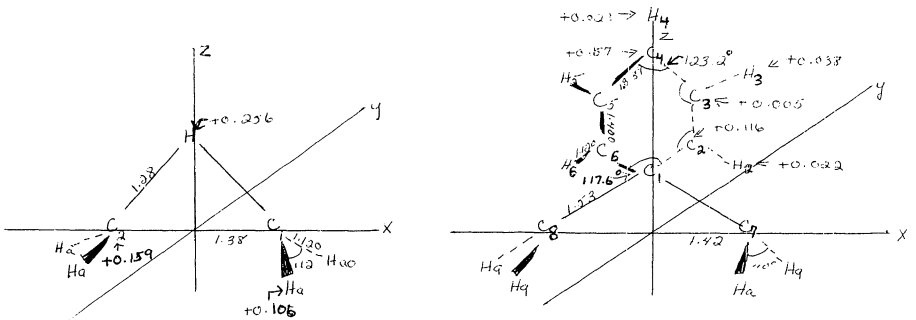

Figure 26. Optimized bridged ethyl and phenonium cations. Charge densities are underlined. Bond C_1Ha in the ethyl cation makes an angle of 3.5° with the plane containing the C_1C_2 bond and is perpendicular to the plane of the three-member ring. The C_7Ha bond in the phenonium ion makes an angle of 13° with the plane containing the C_7C_8 bond and is perpendicular to the 3-member ring.

The 3-member ring in the phenonium ion resembles protonated cyclopropane more than the bridged ethyl cation. Thus a better reference system for the phenonium ion might be protonated cyclopropane. Figure 27 indicates comparable CC bond lengths for the "ethylene" C_7C_8 bond length as well as the C_1C_7 and C_1C_8 bonds to the bridging carbon.[65] In both cations the C_1C_7 and C_1C_8 bond lengths are slightly longer than the bond length we calculated for ethane (1.49A°). This suggests that the bond is weaker than a single bond as would be expected from a 3-centered bond. The C_1C_7 bond length in the phenonium ion is shorter than the corresponding side in protonated cyclopropane due to greater electron density between the carbons probably donated by the phenyl ring.

The bond length expected for benzene is intermediate between the INDO ethylene cc distance, 1.31A, and the ethane, 1.49A cc lengths.[15] This yields an expected value of [(1.31 + 1.49)A/2=] 1.40A. Bond lengths C_1C_2 and C_1C_6 are longer (1.429A) than this expected value (1.40A). The bond angle $C_2C_1C_6$ of 117.6° less than expected for benzene, is consistent with this trend toward an sp^3 hybrid state for C_1.

This structure is consistent with ^{13}C NMR data which indicates that the bridging carbon is in an sp^3 hybrid state.[77]

The calculated barrier to conversion of the phenonium ion to the open 2-phenylethyl cation should be greater than the 20 Kcal/mole predicted by Snyder.[33] Complete optimization of the ring, which Snyder did not undertake, results in a lowering of the energy for the bridged cation compared with the Snyder's optimum configuration. In addition it provides insight into the nature of the phenonium ion.

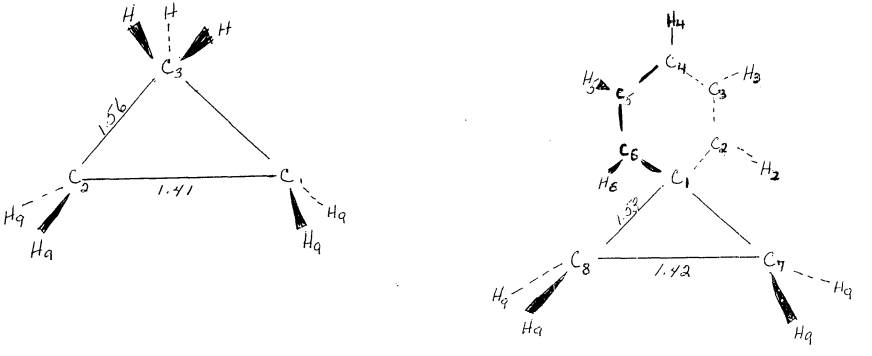

Figure 27. INDO optimized corner-protonated cyctopropyl cation[76] and ethyl phenonium ion.

The "non-classical" ethyl and 2-butyl cations possess 57% and 55% of their total positive charge density within the 3-member ring, respectively (see table 18). It was noted in the discussion in the sec-butyl cation section, the increase in electron density with respect to the ethyl cation within the ring is contributed by the methyl groups through hyperconjugation. The percentage of positive charge in the 3-membered ring drops to 31% in the phenonium ion. This is about half the charge in the ethyl and butyl cations, mentioned above, and about 25% less than the cyclopropyl cation. This is consistent with the greater stability of the 2-phenylethyl cation.

In the phenonium ion most of the positive charge has been delocalized into the benzene ring (61% of the total positive charge residing there). In addition, the positions with the greatest share of this positive charge are the ortho positions, 45% (each positive has 22.5%) and the para position, 29%. The meta positions have 14% of the positive charge (7% at each of the two equivalent meta positions).

This agrees with recent INDO work in this lab[81] and other semiempirical SCF calculations[82] on the benzenium ion (figure 28). The charge distribution is in accord with the general dispersal of charge expected based upon resonance delocalization arguments.[83] It correlates with NMR studies.[84,85]

The orientation of the benzene ring perpendicular to the plane of the 3-member ring in the optimized phenonium ions allows for minimization of repulsion between the ring, and the ring protons with the "ethylene" carbon and hydrogen atoms. This orientation also allows for optimum overlap between the π-system of the ring and the $2p_z(\pi)$ orbitals of C_7 and C_8 of the "ethylene" nucleus.

BRIDGED CATION	ETHYL	2-BUTYL	CYCLOPROPYL[a]	PHENONIUM[b]
% Charge density in 3-member ring	57	55	42	31

a.) Ref. 20

b.) 61% of charge density is the benzene ring

Table 18. INDO calculated charge densities within the 3-member rings of the bridged ethyl, sec-butyl, cyclopropyl and β-phenylethyl cations.

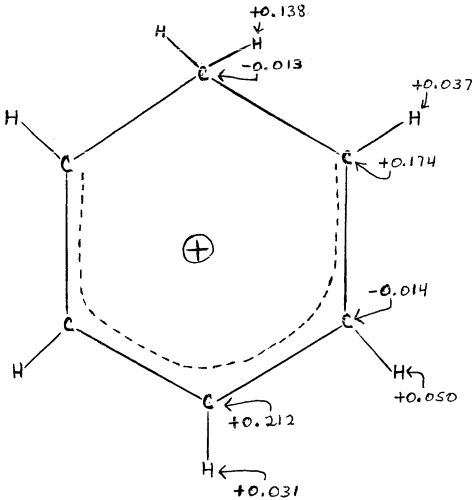

Figure 28. Calculated Charge Densities for the Benzenium Ion.

Syn-anti Isomerization of double bonded nitrogen in free guanidines have been observed [86,87,88,89] by their temperature dependent n.m.r. spectra. Kessler and co-workers[86,87] have shown convincingly that this syn-anti conversion is a true inversion process involving an sp hybridized nitrogen atom in the transition state.

A similar n.m.r. temperature dependence has been observed for the salts of 2-aryl-1,1,3,3-tetramethylguanidine.[87] Two mechanisms have been proposed: (1) a rotation about C---N bond or, (2) deprotonation to the free guanidine followed by inversion and protonation. We considered rotation about the C --- N bond to be more likely on three grounds: (1) in tetramethyl-2-alkylguanidine salts[90] vicinal coupling of the NH-protons with the α protons of the alkyl group occurs at room temperature while simultaneously the signal of the dimethylamino protons appear as a sharp singlet, (2) the free energy of activation of proton exchange was shown to be larger than the free energy of activation for the syn-anti conversion, and (3) they reported finding similar free energy of activation barriers for pentamethylarylguanidine iodide salts.

In the course of our studies of highly substituted guanidines and guanidine salts we found similar rotation barriers. In this report we wish to present the results of our n.m.r. studies and their implications concerning a new aspect of the structure of highly substituted guanidine salts.

Due to its inherent symmetry, NMR rotation barrier studies of the guandinium ion are not feasible. We decided to study this barrier theoretically employing the semiempirical INDO method.[8]

METHOD

General - N.m.r. spectra were obtained with a Varian A60a in-

strument. Deuterochloroform was used as solvent and tetramethylsilane as internal calibrant. Temperature calibration was effected by the usual technique of measuring the separation of methanol resonances. The temperature was determined both before and after each spectra determination.

Preparation of 2,2-diaryl-1,1,3, tetramethylguanidine chlorides. -0.1 mole of the benzyl chloride ($ArCH_2X$) is dissolved in 150 ml of benzene. To this solution is added 0.1 mole of tetramethylguanidine, the flask stoppered and allowed to stand at room temperature for approximately 24 hours. The crystalline precipitate (P_1) is filtered off and the filtrate evaporated down to approximately 10 ml on a rotary evaporator. The crystalline solid (P_2) formed on evaporation is filtered from the remaining liquid and washed with a small quantity of cold benzene. Both P_1 and P_2 are then subjected to fractional recrystallization from o-dichlorobenzene. The products from P_1 and P_2 are combined and recrystallized from o-dichlorobenzene. This final product is then vacuum dried with warming for 24 hours.

Preparation of 2-aryl-1,1,3,3-tetramethylguanidine chloride. -0.2 mole of TMG is dissolved in 100 ml of benzene. To this is added slowly a solution of 0.1 mole of benzyl chloride in 50 ml of benzene the flask stoppered and allowed to stand for 24 hours. The separation procedure is as described above.

The unoptimized guanidinium ion was positioned in the x-y plane as indicated in figure 29. It was assumed that the coordinates of the amino group in quadrant II could be gotten from those of the amino group in quadrant I by multiplying their abscissae by minus 1. The remaining amino group was assumed to be symmetrical with respect to the y axis. The π-system was thus parallel to the z-axis. All CN bond lengths were assumed to be equal as were all N-H bond lengths. All HNH angles were assumed equal.

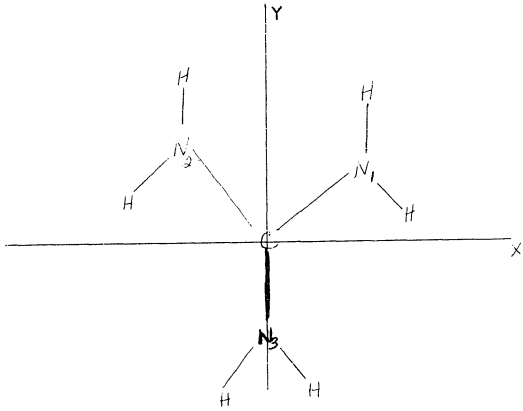

Figure 29. Unoptimized Structure of Guanidinium ion - All Planar.

All bond lengths and bond angles were varied, subject to the above restrictions, to optimize the geometry. The procedure is described in the Optimization Techniques section.

The optimized planar structure was subjected to a rotation to obtain the barrier. Energies were calculated for each rotamer at 5° intervals.

RESULTS

The synthesis of the hexasubstituted guanidine halides is outlined in Figure 30.

The reaction, carried out in benzene, is quite exothermic and goes essentially to completion without heating of the reaction mixture. Under these conditions the guanidine salts precipitate from the reaction mixture as fine needles. If the reaction is carried out with equal molar quantities of tetramethylguanidine (TMG) (XXX) and benzyl halide, the precipitate consists of an approximately equal mixture of (XXXIV) and (XXXIII). Molar ratios of TMG/benzyl halide greater than 1 afford a crystalline mixture of (XXXIV), (XXXIII) and (XXXI), from which (XXXI) can be isolated by fractional crystallization. Although a detailed study of the reaction was not carried out, presumably the predominance of product (XXXIV) over that of (XXXI) is due to reaction III being essentially irreversible and more rapid than reaction I. Increasing the concentration of TMG would tend to favor the formation of (XXXI) by increasing the rate of reaction I relative to reaction II. The following compounds were prepared and their n.m.r. examined (figure 31).

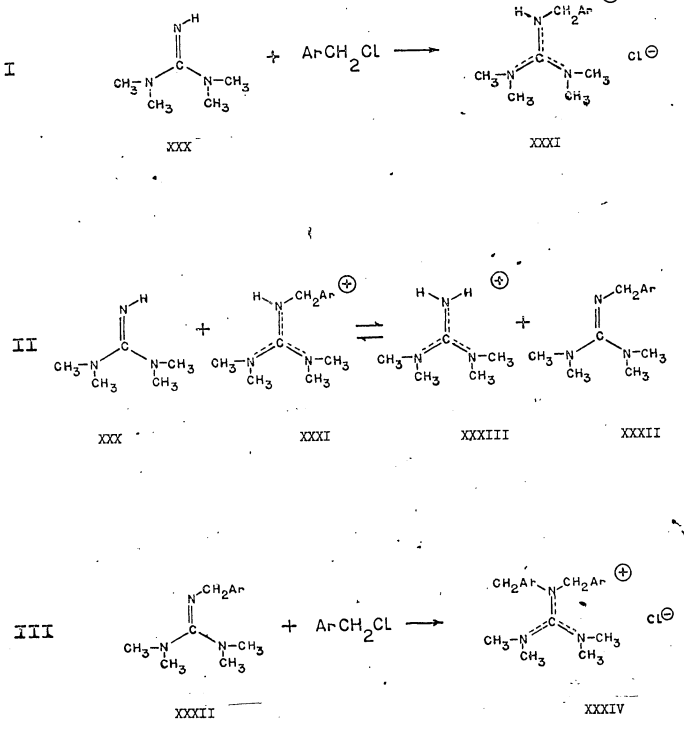

Figure 30

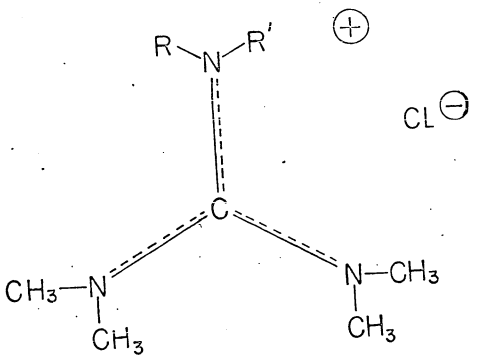

XXXIV a, R=R'= -$CH_2-\phi$

XXXIV b, R=R'= -CH_2-(p-CH_3-C_6H_4)

XXXIV c, R=R'= -CH_2-(o-CH_3-C_6H_4)

XXXIV d, R=R'= -CH_2-(m-CH_3-C_6H_4)

XXXI a, R=H, R'= -$CH_2-\phi$

Figure 31

N.m.r. spectra were determined at various temperatures in deuterochloroform with the objective of detecting restricted rotation and simultaneously determining the associated free energy of activation ($\Delta G^{\ddagger}$). In all cases, we found two temperature dependent peaks, one corresponding to the benzyl hydrogens ($N-CH_2-Ar$) and the other to the N-methyl hydrogens. The benzyl hydrogens show a somewhat broadened singlet at higher temperatures and a broad AB pattern at lower temperatures. The $N-CH_3$ hydrogens, on the other hand, exhibit a sharp singlet at high temperatures which degnerates to two overlapping singlets at lower temperatures. Compound XXXIa, an exception shows only a broadening of the $N-CH_3$ hydrogens at the lowest temperature achievable in our experiment but otherwise still exhibits at typical AB pattern at lower temperatures for the benzyl hydrogens.

The coalescence temperatures, chemical shifts and values are summarized in Table 19. Figure 32, shows two typical N.m.r. spectra at room temperature and the temperature dependence of both the $N-CH_2Ar$ and $N-CH_3$ resonances. Assignment of the resonances is based on their relative area and their chemical shift with respect to TMS. The free energies of activation were calculated by means of the familiar Eyring equation.

The optimized geometry of the guanidinium ion is summarized in Table 20 and Figure 33. The charge densities are listed in Table 21 and Figure 33.

The charge densities are in agreement with ESCA data. The D_{3h} symmetry determined for the molecules is as expected.

Table 19

COMPOUND	$-N(CH_3)_2$			$-N(CH_2Ar)_2$		
	TEMP. °K	$\Delta\nu$ Hz	$\Delta G^{\ddagger}$ KCAL/MOLE	TEMP. °K	$\Delta\nu$ Hz	$\Delta G^{\ddagger}$ KCAL/MOLE
XXXIVa	276.0	3.0	14.5	290.0	22.3	14.1
XXXIVb	298.7	4.0	15.7	312.0	17.2	15.5
XXXIVc	298.0	3.5	15.7	307.0	19.2	15.1
XXXIVd	297.0	9.0	15.1	302.5	18.6	14.9
XXXI a	——	—	—	285.0	16.4	14.1

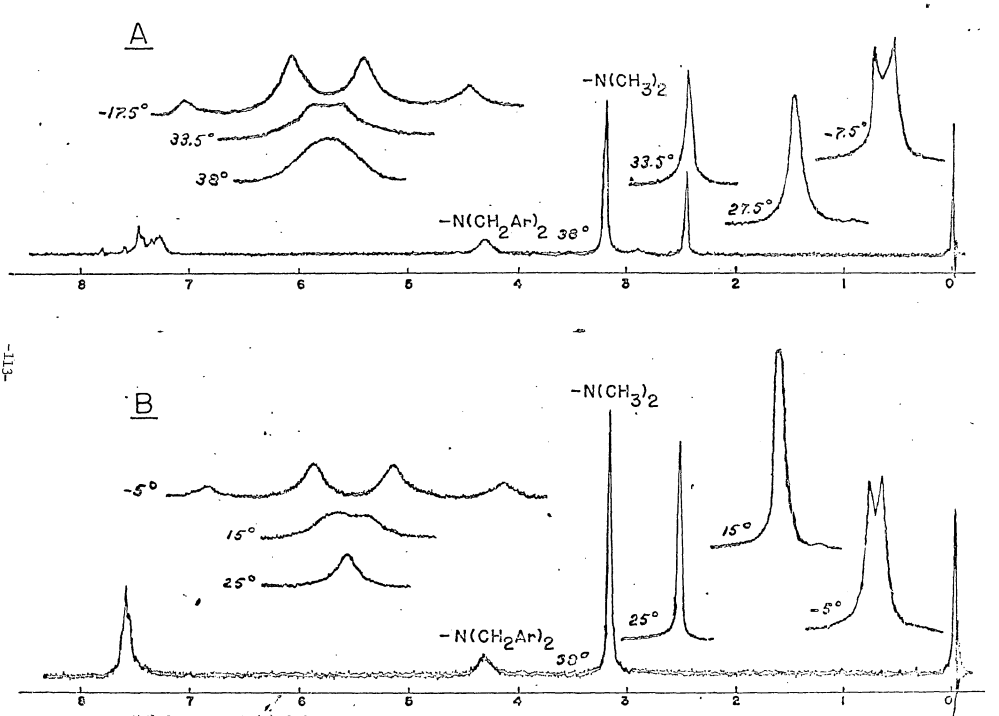

FIG. 32 NMR Spectra of (A) 2,2-di-m-xylyl-1,1,3,3-tetramethyl guanidine chloride and (B) 2,2-dibenzyl-1,1,3,3-tetramethyl guanidine chloride.

BOND LENGTHS (A°)		BOND ANGLES (DEGREES)	
CN	NH	NCN	CNH
1.300	1.070	120.0	124.0

Table 20. INDO Optimized geometry of the guanidinium ion.

N	C	H
-0.2120	+0.5465	+0.1816

Table 21. INDO calculated charge densities for the guanidinium ion.

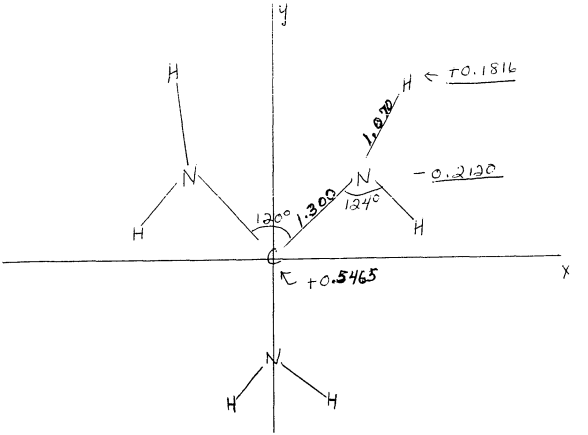

Figure 33. INDO optimized guanidinium ion geometry and charge densities (underlined)

The rotational energy vs. angle of rotation is plotted in figure 34. The calculated four-fold barrier to rotation for the guanidinium ion is 24 Kcal/mole.

DISCUSSION

At low temperatures the $-N(CH_3)_2$ resonances appear at different chemical shifts due to their "syn-anti" relationship with respect to the $-N(CH_2AR)_2$ groups in the apparent planar structure (see figure 35).

As suggested by Kessler [87], the interconversion of the syn-anti methyls at higher temperatures must obviously involve a rotation about the (a) bonds. It should be noted that the free energy of activiation barriers are of the same magnitude as those found by Kessler [87] for tetramethylaryl guanidine salts.

More interesting is the temperature dependence of the benzyl hydrogen resonance. There are three possible in interpretations of this behavior: (1) restricted rotation about bond (c) is capable of creating an asymmetric environment which renders the benzyl hydrogens non-equivalent. (2) similarly, restricted rotation about bond (d) could lead to the same type of nonequivalence. (3) finally, let us assume that rotation about bond(b) is restricted and the $-N(CH_2Ar)_2$ group is not in nor perpendicular to the plane of the guanidine nucleus. If such is the case, regardless of rapid rotation about bonds (c) and (d) the benzyl hydrogens will not be equivalent and a single AB spectrum should arise.

Mechanism (3) seems most likely on several gounds. Dreiding models indicate that their would be little if any steric interference to rotations about bonds (c) and (d). If so, the free energy of activation barriers would be an order of magnitude lower than the measured

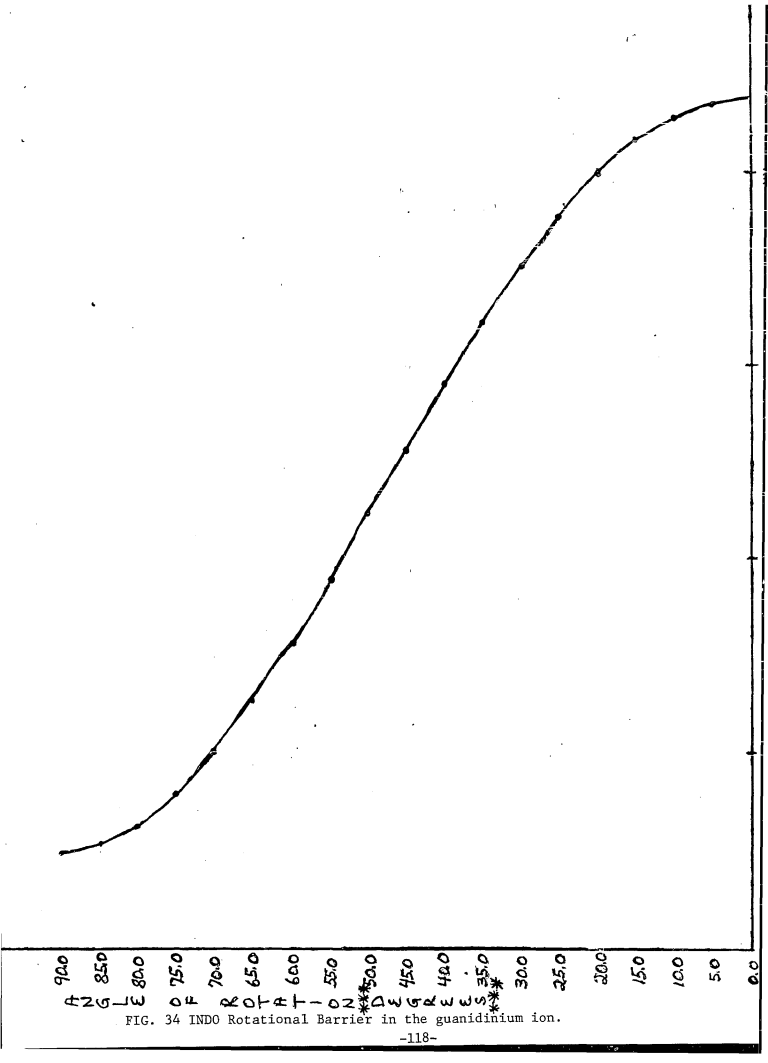

FIG. 34 INDO Rotational Barrier in the guanidinium ion.

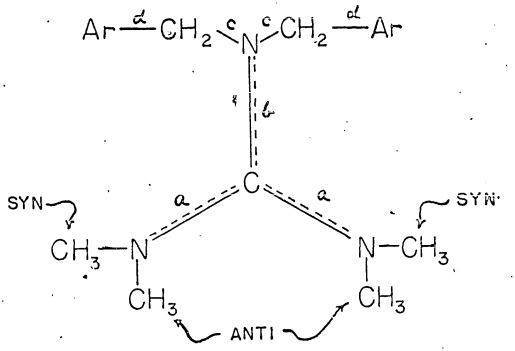

Figure. 35- Syn-anti relationshp of $-N(CH_3)_2$ groups and possible restricted rotations.

values. Secondly, if mechanisms (1) or (2) were operative, substitution in the ortho positon would significantly change the free energy of activation. We found no significant difference in the $\Delta G^{\ddagger}$ values for the ortho (XXXIVd), meta (XXXIVc) and para (XXXIVb) 2,2-dixylyl-1,1,3-3-tetramethyl guanidine cations. In addition, mechanism (1) seems unlikely since both 2-benzyl-1,1,3,3-tetramethylguanidine chloride (XXX1a) and 2,2-dibenzyl-1,1,3,3-tetramethylguanidine chloride (5a) have the same $\Delta G^{\ddagger}$ values which is unexpected on steric grounds.

Drieding models, on the other hand, suggest significant steric crowding in the planar structure which can be relieved by a slight rotation about bonds (a) and (b). Small rotations about these bonds would not however, significantly reduce the delocalization energy of the guanidine structure. We are, therefore, led to the conclusion that a propeller-like stable conformation must exist for these cations. (see figure 36). On the basis of such a model, one would expect little if any difference in the $\Delta G^{\ddagger}$ values for the $-N(CH_3)_2$ and $-N(CH_2Ar)_2$ groups. An examination of table 19 shows that such is the case for those compounds studied.

We, therefore, conclude that highly substituted guanidine cations are non-planar, probably existing at low temperatures in asymmetric propeller like conformation. Secondly, unless steric interference between substituents bound to nitrogen is large, stabilization due to electron delocalization should still be substantial.

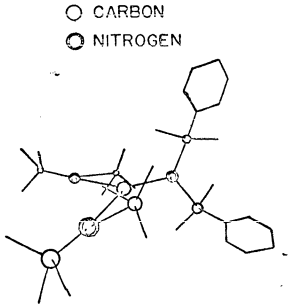

Figure 36. Conformation of 2,2-dibenzyl-1,1,3,3-tetramethylguanidine cation.

Appendix. Sample INDO Output

```
 ETHYLENE + H+ C=C 1.37  H-Z=1.1
INDO CLOSED

        7 ATOMS   CHARGE =   1   MULTIPLICITY =   1   IUNITS =   0

   1     -0.0000000      -0.0000000       1.1000000
   6       .6850000      -0.0000000      -0.0000000
   1      1.2489505       .9269264      -0.0000000
   1      1.2489505      -.9269264      -0.0000000
   6      -.6850000      -0.0000000      -0.0000000
   1     -1.2489505      -.9269264      -0.0000000
   1     -1.2489505       .9269264      -0.0000000
IN INTCV
IN CCEFF
IN INTGRL
```

OVERLAP INTEGRAL MATRIX

	1	2	3	4	5	6	7	8	9	10	11
1	1.0000	.4095	-.2209	0.0000	.3547	.1535	.1535	.4095	.2209	0.0000	.3547
2	.4095	1.0000	0.0000	0.0000	0.0000	.5217	.5217	.4215	.4231	0.0000	0.0000
3	-.2209	0.0000	1.0000	0.0000	0.0000	.2547	.2547	-.4231	-.3286	0.0000	0.0000
4	0.0000	0.0000	0.0000	1.0000	0.0000	.4187	-.4187	0.0000	0.0000	0.0000	0.0000
5	.3547	0.0000	0.0000	0.0000	1.0000	0.0000	0.0000	0.0000	0.0000	0.0000	.2569
6	.1535	.5217	.2547	.4187	0.0000	1.0000	.1657	.1210	.1326	.0636	0.0000
7	.1535	.5217	.2547	-.4187	0.0000	.1657	1.0000	.1210	.1326	-.0636	0.0000
8	.4095	.4215	-.4231	0.0000	0.0000	.1210	.1210	1.0000	0.0000	0.0000	0.0000
9	.2209	.4231	-.3286	0.0000	0.0000	.1326	.1326	0.0000	1.0000	0.0000	0.0000
10	0.0000	0.0000	0.0000	.2569	0.0000	.0636	-.0636	0.0000	0.0000	1.0000	0.0000
11	.3547	0.0000	0.0000	0.0000	.2569	0.0000	0.0000	0.0000	0.0000	0.0000	1.0000
12	.1535	.1210	-.1326	-.0636	0.0000	.0213	.0602	.5217	-.2547	-.4187	0.0000
13	.1535	.1210	-.1326	.0636	0.0000	.0602	.0213	.5217	-.2547	.4187	0.0000

	12	13
1	.1535	.1535
2	.1210	.1210
3	-.1326	-.1326
4	-.0636	.0636
5	0.0000	0.0000
6	.0213	.0602
7	.0602	.0213
8	.5217	.5217
9	-.2547	-.2547
10	-.4187	.4187
11	0.0000	0.0000
12	1.0000	.1657
13	.1657	1.0000

COULOMB INTEGRAL MATRIX

	1	2	3	4	5	6	7
1	.7500	.3847	.2761	.2761	.3847	.2761	.2761
2	.3847	.5903	.4355	.4355	.3629	.2459	.2459
3	.2761	.4355	.7500	.2834	.2459	.1701	.2117
4	.2761	.4355	.2834	.7500	.2459	.2117	.1701
5	.3847	.3629	.2459	.2459	.5903	.4355	.4355
6	.2761	.2459	.1701	.2117	.4355	.7500	.2834
7	.2761	.2459	.2117	.1701	.4355	.2834	.7500

IN SCF

IN HLCKCL
CORE HAMILTONIAN

IN SCFCL

ELECTRCNIC ENERGY -40.6889675065

ELECTRCNIC ENERGY -40.7094926888

ELECTRCNIC ENERGY -40.7101271886

ELECTRCNIC ENERGY -40.7101731157

ELECTRCNIC ENERGY -40.7101769486

ELECTRCNIC ENERGY -40.7101772830
ENERGY SATISFIED

HARTREE-FOCK ENERGY MATRIX
EIGENVALUES AND EIGENVECTORS

				EIGENVALUES---	-1.9482	-1.3723	-1.2673	-1.1281	-1.0441	-.9269	-.1666	-.1192	-.0886	-.0512
					1	2	3	4	5	6	7	8	9	10
1	1	H	S		.3360	.0000	-.0000	-.4695	.1950	-.0000	.0000	-.7879	.0000	.0000
2	2	C	S		.5684	-.4421	.0000	.1601	-.0348	.0000	.0115	.0960	.5014	-.0000
3	2	C	PX		-.2084	-.3299	.0000	.2781	.5223	-.0000	.0154	-.1576	-.0029	-.0000
4	2	C	PY		-.0000	.0000	.5613	-.0000	-.0000	-.4544	.0000	.0000	.0000	-.4300
5	2	C	PZ		.0661	-.0029	-.0000	-.4555	.3699	.0000	.7063	.3878	-.0275	.0000
6	3	H	S		.1907	-.3133	.3041	.1991	.1872	-.3831	-.0194	.0507	-.3521	.3969
7	4	H	S		.1907	-.3133	-.3041	.1991	.1872	.3831	-.0194	.0507	-.3521	-.3969
8	5	C	S		.5684	.4421	.0000	.1601	-.0348	-.0000	-.0115	.0960	-.5014	-.0000
9	5	C	PX		.2084	-.3299	-.0000	-.2781	-.5223	.0000	.0154	.1576	-.0029	.0000
10	5	C	PY		.0000	.0000	.5613	-.0000	.0000	.4544	.0000	-.0000	.0000	-.4300
11	5	C	PZ		.0661	.0029	.0000	-.4555	.3699	.0000	-.7063	.3878	.0275	-.0000
12	6	H	S		.1907	.3133	-.3041	.1991	.1872	-.3831	.0194	.0507	.3521	-.3969
13	7	H	S		.1907	.3133	.3041	.1991	.1872	.3831	.0194	.0507	.3521	.3969

				EIGENVALUES---	.0691	.1077
					12	13
1	1	H	S		-.0000	.0000
2	2	C	S		.0000	.2303
3	2	C	PX		-.0000	-.6258
4	2	C	PY		.5413	-.0000
5	2	C	PZ		.0000	.0190
6	3	H	S		-.3213	.1658
7	4	H	S		.3213	.1658
8	5	C	S		-.0000	-.2303
9	5	C	PX		-.0000	-.6258
10	5	C	PY		-.5413	.0000
11	5	C	PZ		-.0000	-.0190
12	6	H	S		-.3213	-.1658
13	7	H	S		.3213	-.1658

IN CRRINT
DENSITY MATRIX

				1	2	3	4	5	6	7	8	9	10
1	1	H	S	.7426	.2181	-.1975	.0000	.6164	.0142	.0142	.2181	.1975	-.0000
2	2	C	S	.2181	1.0907	.1067	-.0000	-.0939	.5445	.5445	.3089	.4750	.0000
3	2	C	PX	-.1975	.1067	1.0035	.0000	.1074	.4330	.4330	-.4750	-.5709	-.0000
4	2	C	PY	.0000	-.0000	.0000	1.0432	-.0000	.6895	-.6895	.0000	-.0000	.2172
5	2	C	PZ	.6164	-.0939	.1074	-.0000	.6975	-.0159	-.0159	-.0990	-.1036	.0000
6	3	H	S	.0142	.5445	.4330	.6895	-.0159	.8969	-.0599	-.0096	-.0208	-.0068
7	4	H	S	.0142	.5445	.4330	-.6895	-.0159	-.0599	.8969	-.0096	-.0208	.0068
8	5	C	S	.2181	.3089	-.4750	.0000	-.0990	-.0096	-.0096	1.0927	-.1067	.0000
9	5	C	PX	.1975	.4750	-.5709	-.0000	-.1036	-.0208	-.0208	-.1067	1.0035	-.0000
10	5	C	PY	-.0000	.0000	-.0000	.2172	.0000	-.0068	.0068	.0000	-.0000	1.0432
11	5	C	PZ	.6164	-.0990	.1036	-.0000	.6974	-.0195	-.0195	-.0939	-.1074	.0000
12	6	H	S	.0142	-.0096	.0208	.0068	-.0195	.1344	-.0828	.5445	-.4330	-.6895
13	7	H	S	.0142	-.0096	.0208	-.0068	-.0195	-.0828	.1344	.5445	-.4330	.6895

				12	13
1	1	H	S	.0142	.0142
2	2	C	S	-.0096	-.0096
3	2	C	PX	.0208	.0208
4	2	C	PY	.0068	-.0068
5	2	C	PZ	-.0195	-.0195
6	3	H	S	.1344	-.0828
7	4	H	S	-.0828	.1344
8	5	C	S	.5445	.5445
9	5	C	PX	-.4330	-.4330
10	5	C	PY	-.6895	.6895
11	5	C	PZ	-.0159	-.0159
12	6	H	S	.8969	-.0599
13	7	H	S	-.0599	.8969

TOTAL ENERGY = -17.0461360749

BINDING ENERGY= -2.0095751917 A.U.

1	H	.7426	.2574	.0000
2	C	3.8349	.1651	.2065
3	H	.8969	.1031	.1468
4	H	.8969	.1031	.1468
5	C	3.8349	.1651	.2065
6	H	.8969	.1031	.1468
7	H	.8969	.1031	.1468

*DIPOLE MOMENTS

COMPONENTS	X	Y	Z
DENSITIES	-.00000	.00000	1.35989
S,P	.00000	.00000	.84804
P,D	0.00000	0.00000	0.00000
TOTAL	.00000	.00000	2.20793

DIPOLE MOMENT= 2.20793 DEBYES

REFERENCES

1. For reviews of the field see:
   a. D. Bethel and V. Gold, Carbonium Ions: An Introduction, Academic Press, New York, 1967
   b. G. A. Olah and P.v.R. Schleyer, Ed., Carbonium Ions, vol. I, II, III, IV, Wiley Interscience, New York, 1968, 1970, 1972, 1973.
   c. P. D. Bartlett, Ed., Non-classical Ions, W. A. Benjamin, New York, 1965.
   d. S. P. McManus and C. U. Pittman, Jr., Organic Reactive Intermediates, S.P. McManus, Ed., Academic Press, New York, 1973 p. 193.

2. G. A. Olah, Angewandte Chemie (Eng.), 12, 173 (1973).

3. R. Hoffmann, J. Chem. Phys., 40, 2480 (1964).

4. R. Hoffmann, J. Chem. Phys., 39, 1397 (1963).

5. M. J. S. Dewar, The Molecular Orbital Theory of Organic Chemistry, McGraw-Hill Book Co., New York, 1969, pg. 443.

6. J. A. Pople, D.P. Santry and G. A. Segal, J. Chem. Phys., 43, S129 (1965).

7. J. A. Pople, and G. A. Segal, J. Chem. Phys., 44, 3289 (1966).

8. J. A. Pople, D. L. Beveridge and P. A. Dobosh, J. Chem. Phys., 47, 2027 (1967).

9. M. S. Gordon and J. A. Pople, J. Chem. Phys., 49, 4643 (1968).

10. J. A. Pople and M. S. Gordon, J. Am. Chem. Soc., 89 4253 (1967).

11. M. S. Gordon and H. Fischer, J. Am. Chem. Soc., 90, 2471 (1968).

12. M. S. Gordon and R. D. Koob, J. Am. Chem. Soc., 93, 4649 (1971).

13. R. Sustmann, J. E. Williams, M. J. S. Dewar, L. C. Allen and P.v.R. Schleyer, J. Am. Chem. Soc., 91, 5350 (1969).

14. L. Massa, private communication.

15. J. J. Dannenberg and T. D. Berke: 158th National American Chemical Society Meeting, New York, September 1969, Abstract Phys., 163 and unpublished results.

16. L. Radom, J. A. Pople, V. Buss, P.v.R. Schleyer, J. Am. Chem. Soc., 93, 1813 (1971).

17. W. J. Hehre, R. F. Stewart and J. A. Pople, J. Chem. Phys., 51, 2657 (1969).

18. R. Ditchfield, W. J. Hehre and J. A. Pople, J. Chem. Phys., 54 724 (1971).

19. L. Radom, J. A. Pople, V. Buss, and P.v.R. Schleyer, J. Am. Chem. Soc., 94, 311 (1972).

20. M. J. S. Dewar, N. Bodor and D. Lo, J. Am. Chem. Soc., 94, 5303 (1972).

21. For reviews see:
    a. J. L. Beauchamp, Am. Rev. Phys. Chem., 22, 527 (1971)
    b. J. D. Baldschweiler, Carbonium Ions, Vol. III, G. A. Olah and P.v.R. Schleyer, Ed., Wiley-Interscience, New York 1972 and p. 413, and articles by
    c. H. H. Jaffe and S. Billets, J. Am. Chem. Soc., 94, 674 (1972)
    d. H. H. Jaffe, S. Billets and F. Kaplan, Org. Mass Spec., 7, 431 (1973).

22 a. R. J. Blint, T. B. McMahon and J. L. Beauchamp, J. Am. Chem. Soc., 96, 1269 (1974).

    b. J. L. Beauchamp, D. Holtz, S. D. Woodgate and S. L. Patt, J. Am. Chem. Soc., 94, 2798 (1972).

23. a. F. W. McLafferty, Ed., Mass Spectrometry of Organic Ions, Academic Press, New York, 1963.
    b. M. M. Barsey and F. W. McLafferty, Carbonium Ions, Vol. I, G. A. Olah and P.v.R. Schleyer, Ed., Wiley-Interscience, New York, 1968, p. 257.
    c. P. Ausloos, R. E. Rebbert, L. W. Sieck, T. O. Tiernem, J. Am. Chem. Soc., 94, 8939 (1972).

24. J. T. Keating and P. S. Skell, Carbonium Ions, Vol. II, G. A. Olah and P.v.R. Schleyer, Ed., Wiley-Interscience, New York, 1970 p. 601.

25. F. L. Schadt and P.v.R. Schleyer, J. Am. Chem. Soc., 95, 7860 (1973).

26. J. A. Pople, D. L. Beveridge and P. A. Dobosh, J. Am. Chem. Soc., 90, 4201 (1968).

27. R. G. Parr, J. Chem. Phys., 20, 239 (1952).

28. For reviews of semiempirical techniques see:
    a. J. A. Pople and D. L. Beveridge, Approximate Molecular Orbital Theory, McGraw-Hill, New York, 1970.
    b. G. Klopman and B. O'Leary, Introduction to All-Valence Electrons SCF Calculations of Large Organic Molecules, Springer-Verlag, New York, 1970.
    c. J. N. Murrell and H. J. Harget, Semiempirical Self-Consistent-Field Molecular Orbital Theory of Molecules, Wiley-Interscience New York, 1972.
    d. J. A. Pople, D. L. Beveridge and N. S. Ostlund, Int. J. Quant. Chem., 1, 293 (1967).
    e. H. H. Jaffe, Accts. Chem. Res., 2, 136 (1969).
    f. J. A. Pople, Accts. Chem. Res., 3, 217 (1970).

29. C. C. J. Roothaan, Rev. Mod. Phys., 23, 69 (1951).

30. M. Geoppert-Mayer and A. L. Sklar, J. Chem., Phys., 6, 645 (1938).

31. J. C. Slater, Quantum Theory of Atomic Structure, McGraw-Hill, New York, 1960, Vol., I, p. 339.

32. a. J. A. Pople, J. W. McIver, Jr., and N. S. Ostlund, Chem. Phys. Lett., 1, 465 (1967).
    b. J. A. Pople, J. W. McIver, Jr., and N. S. Ostlund, J. Chem. Phys., 49, 2965 (1968).
    c. G. E. Bloor and D. L. Breen, J. Am. Chem. Soc., 89, 6832 (1967).
    d. G. E. Bloor and D. L. Breen, J. Chem. Phys., 72, 716 (1968).

33. E. I. Snyder, J. Am. Chem. Soc., 92, 7529 (1970).

34. K. B.Wiberg, J. Am. Chem. Soc., 90, 59 (1968).

35. L. Radom, W. A. Latham, W. J. Hehre, J. A. Pople, J. Am. Chem. Soc., 93, 5339 (1971).

36. P. C. Hariharan and J. A. Pople, Chem. Phys. Lett., 16, 217 (1972).

37. L. E. Sutton, Ed., Tables of Interatomic Distances and Configurations in Molecules and Ions, Special Publication No. 11, The Chemical Society, London, 1968.

38. P. C. Hariaharan, W. A. Latham and J. A. Pople, Chem. Phys. Lett., 14, 385 (1972).

39. P. C. Hariharan, L. Radom, J. A. Pople, P.v.R. Schleyer, J. Am. Chem. Soc., 96, 599 (1974).

40. B. Zurawski, R. Ahlrichs and W. Ketzelnigg, Chem. Phys. Lett., 21 309 (1973).

41. "Non-classical" - the term coined by Roberts and Lee[42] referring to bridged (tetracoordinated) or 3-center bond systems.

42. J. D. Roberts and C. C. Lee, J. Am. Chem. Soc., 73, 5009 (1951).

43. J. D. Roberts and J. A. Yancey, J. Am. Chem. Soc., 74, 5943 (1952).

44. P. C. Myhre and E. Evans, J. Am. Chem. Soc., 91, 5641 (1969).

45. V. J. Shiner, Jr. and J. O. Stoeffer, J. Am. Chem. Soc., 92, 3191 (1970).

46. V. J.Shiner, Jr. and J. G. Jewett, J. Am. Chem. Soc., 86, 945 (1964).

47. a. J. J. Dannenberg, D. H. Weinwurzel, K. Dill and B. J.Goldberg Tetrahedron Lett. 13, 124 (1972).
b. J. J. Dannenberg, B. J. Goldberg, J. K. Barton, K. Dill, D. H. Weinwurzel and M. O. Longas, in press.

48. a. H. Kollmar and H. O. Smith, Theoret. Chem. Acta. 20, 65 (1971).
b. H. Kollmar and H. O., Agnew Chem.(Eng.), 9, 462 (1970).

49. a. J. M. Lehn and G. Wipff, J. C. S. Chem. Comm., 747 (1973).
b. D. T. Clark and D. H. Lilley, J. C. S. Chem. Comm., 549 (1970).
c. D. T. Clark and D. H. Lilley, Tetrahedron, 29, 845 (1973).
d. D. A. Dixon and W. N. Lipscomb, J. Am. Chem. Soc., 95, 2853 (1973).

50. Tables of Interatomic Distances and Configurations in Molecules and Ions, Supplement 1956-59, Special Publication No. 18, The Chemical Society, London, 1965.

51. See for example:
a. R. C. Fahey and C. A. McPherson, J. Am. Chem. Soc., 91, 3865 (1969).
b. R. Breslow, Organic Reaction Mechanisms, Benjamin, New York, 1966, p. 114.
c. J. D. Roberts and M. C. Caserio, Basic Principals of Organic Chemistry, Benjamin, New York, 1964, p. 179.

52. M. J. S. Dewar and A. P. Marchand, Ann. Rev. Phys. Chem., 16,321 (1961) review article.

53. H.Fischer and H. Kollmar, Theoret. Chem. Acta. 13, 213 (1969).

54. J. E. Williams, Jr., V. Buss, L. C. Allen, P.v.R. Schleyer, W. A. Lathan, W. J. Hehre, J. A. Pople, J. Am. Chem. Soc., 92, 2141 (1970).

55. W. J. Lafferty, E. K. Plyer and E. D.Tidwell, J. Chem. Phys., 37, 1981 (1962).

56. G. A. Olah, Carbocations and Electrophilic Reactions, John Wiely New York (1974), p. 12.

57. C. D. Nenitzescu, Carbonium Ions, Vol., I, G. A. Olah and P.v.R. Schleyer, Ed., Wiley-Interscience, New York, 1968, p. 64.

58. J. D. Roberts, W. Bennett, R. E. McMahon, and W. E. Holroyd, Jr., J. Am. Chem., Soc., 74, 4283 (1952).

59. M. Saunders, E. L. Hagen and J. Rosenfeld, J. Am. Chem. Soc., 90, 6822 (1968).

60. a. Magic Acid[R] is a registered trademark of Cationics, Inc.
b. A. Commeyras and G. A. Olah, J. Am. Chem. Soc., 91, 2929 (1969).

61. G. A. Olah and A. M. White, J. Am. Chem. Soc., 91, 5801 (1969).

62. J. B. Stothers, Carbon-13 NMR Spectroscopy, Academic Press, New York 1972, Chapter 6.

63. a. W. A. Lathan, W. J. Hehre and J. A. Pople, J. Am. Chem. Soc., 93, 808 (1971).
b. L. Radom, J. A. Pople and P.v.R. Schleyer, J. Am. Chem. Soc., 94, 5935 (1972).

64. J. J. Dannenberg and T. D. Berke, Theoret. Chem. Acta (Berl.) 24, 99 (1972).

65. It should be noted that the CNDO method (therefore presumably the INDO method) favors small ring structures over open chain isomers.[30] This may very well be due to neglect of 3- and 4-center repulsive interactions in the method. Nevertheless, a comparison between two analogous cyclic structures is less likely to encounter problems of this nature.

66. N. C. Baird, Theoret. Chem. Acta. (Berl), 16, 239 (1970).

67. For a review see:
C. J. Lancelot, D. J. Cram and P.v.R. Schleyer, Carbonium Ions, Vol. III, G. A. Olah and P.v.R. Schlery, Ed., Wiley-Interscience New York, 1972, p. 1347.

68. a. D. J. Cram, J. Am. Chem. Soc., 71, 3863 (1949) First paper of series.
b. D. J. Cram, J. Am. Chem. Soc., 86, 3767 (1964) Review paper on phenonium ions with references to other papers in the study.

69. Distribution corrected due to racemization occurring 5 times as rapidly as solvolysis in L-threo-3-penyl-2-butyl tosylate.

70. H. C. Brown, The Transition State, special publication No. 16, The Chemical Society, London, London, 1962 p. 140.

71. H. C. Brown, K. J. Morgan and F. J. Chloupek, J. Am. Chem. Soc., 87, 2137 (1965).

72. A. Streitwieser, Jr., Solvolytic Displacement Reactions, McGraw-Hill, New York, 1962, p. 63.

73. S. G. Smith, A. H. Fainberg and S. Winstein, J. Am. Chem. Soc., 83, 618 (1961).

74. J. E. Nordlander and W. G. Deadman, J. Am. Chem. Soc., 90, 1590 (1968).

75. R. J. Jablonski and E. I. Snyder, Tetrahedron Letters, 1103 (1968).

76. J. E. Nordlander and W. J. Kelly, J. Am. Chem. Soc., 91, 996 (1969).

77. G. A. Olah, reg. 52, p. 9.

78. a. J. March, Advanced Organic Chemistry: Reactions, Mechanisms and Structure, McGraw-Hill, New York, 1968, p. 281.
b. R. W. Alder, R. Baker and J. M. Brown, Mechanism in Organic Chemistry, Wiley-Interscience, New York, 1971, ch. 1.

79. J. J. Burke and P. C. Lauterbur, J. Am. Chem. Soc., 86, 1870 (1964).

80. H. Fischer, H. Kollmar and H. O. Smith, Tetrahedron Letters, 55, 5821 (1958).

81. J. J. Dannenberg and A. V. Santoro, in press. It is an INDO level study of electrophilic aromatic substitution.

82. a. J. P. Colpa, C. MacLean and E. L. Mackor, Tetrahedron, 19, Suppl. 2, 65 (1963).
b. C. MacLean and E. L. Mackor, Mol Phys., 4, 241 (1961).
c. N. Muller, L. W. Pickett and R. S. Mulliken, J. Am. Chem. Soc., 76, 4770 (1954).
d. M. Simonetta and E. Heilbronner, Theoret. Chem. Acta. (Berl.) 2, 228 (1964).

83. J. B. Hendrickson, D. J. Cram and G. S. Hammond, Organic Chemistry, 3rd Ed., McGraw-Hill, New York, 1970, p. 653.

84. G. A. Olah, Acct. Chem. Res., 4, 240 (1971).

85. G. A. Olah, R. H. Schlosberg, D. P. Kelly and Gh. D. Mateescu, J. Am. Chem. Soc., 92, 2546 (1970).

86. H. Kessler and D. Leibfritz, Tetrahedron, 25, 5127 (1969).

87. V. J. Bauer, W. Fulmor, G. O. Morton and S. R. Safir, J. Am. Chem. Soc., 90, 6846 (1968).

88. H. Kessler and D. Leibfritz, Tetrahedron, 26, 1805 (1970).

89. H. Kessler, Tetrahedron Letters, 17, 2041 (1968).

90. H. Kessler and D. Leibfritz, Tetrahedron Letters, 427 (1969).